Radiation Detection and Measurement

Third Edition

Glenn F. Knoll
Professor of Nuclear Engineering and Radiological Sciences
University of Michigan
Ann Arbor, Michigan

John Wiley & Sons, Inc.

Chapter 2

Radiation Interactions

The operation of any radiation detector basically depends on the manner in which the radiation to be detected interacts with the material of the detector itself. An understanding of the response of a specific type of detector must therefore be based on a familiarity with the fundamental mechanisms by which radiations interact and lose their energy in matter. Many general reference works are available concerning this broad topic; the classic text by Evans,[1] to mention only one, has served as a standard reference for several decades.

To organize the discussions that follow, it is convenient to arrange the four major categories of radiations introduced in Chapter 1 into the following matrix:

Charged Particulate Radiations		**Uncharged Radiations**
Heavy charged particles (characteristic distance $\cong 10^{-5}$ m)	$\Leftarrow$	Neutrons (characteristic length $\cong 10^{-1}$ m)
Fast electrons (characteristic distance $\cong 10^{-3}$ m)	$\Leftarrow$	X-rays and gamma rays (characteristic length $\cong 10^{-1}$ m)

The entries in the left column represent the charged particulate radiations that, because of the electric charge carried by the particle, continuously interact through the coulomb force with the electrons present in any medium through which they pass. The radiations in the right column are uncharged and therefore are not subject to the coulomb force. Instead, these radiations must first undergo a "catastrophic" interaction (often involving the nucleus of constituent atoms) that radically alters the properties of the incident radiation in a single encounter. In all cases of practical interest, the interaction results in the full or partial transfer of energy of the incident radiation to electrons or nuclei of the constituent atoms, or to charged particle products of nuclear reactions. If the interaction does not occur within the detector, these uncharged radiations (e.g., neutrons or gamma rays) can pass completely through the detector volume without revealing the slightest hint that they were ever there.

The horizontal arrows shown in the diagram illustrate the results of such catastrophic interactions. An X- or gamma ray, through the processes described in this chapter, can transfer all or part of its energy to electrons within the medium. The resulting *secondary electrons* bear a close similarity to the fast electron radiations (such as the beta particle) discussed in Chapter 1. Devices designed to detect gamma rays are tailored to promote such interactions and to fully stop the resulting secondary electrons so that their entire energy may contribute to the output signal. In contrast, neutrons may interact in such a way as to produce secondary heavy charged particles, which then serve as the basis of the detector signal.

Also listed in the diagram are order-of-magnitude numbers for the characteristic distance of penetration or average path length (range or mean free path) in solids for typical energy radiations in each category.

I. INTERACTION OF HEAVY CHARGED PARTICLES

A. Nature of the Interaction

Heavy charged particles, such as the alpha particle, interact with matter primarily through coulomb forces between their positive charge and the negative charge of the orbital electrons within the absorber atoms. Although interactions of the particle with nuclei (as in Rutherford scattering or alpha-particle-induced reactions) are also possible, such encounters occur only rarely and they are not normally significant in the response of radiation detectors. Instead, charged particle detectors must rely on the results of interactions with electrons for their response.

Upon entering any absorbing medium, the charged particle immediately interacts simultaneously with many electrons. In any one such encounter, the electron feels an impulse from the attractive coulomb force as the particle passes its vicinity. Depending on the proximity of the encounter, this impulse may be sufficient either to raise the electron to a higher-lying shell within the absorber atom (*excitation*) or to remove completely the electron from the atom (*ionization*). The energy that is transferred to the electron must come at the expense of the charged particle, and its velocity is therefore decreased as a result of the encounter. The maximum energy that can be transferred from a charged particle of mass m with kinetic energy E to an electron of mass m_0 in a single collision is $4Em_0/m$, or about $1/500$ of the particle energy per nucleon. Because this is a small fraction of the total energy, the primary particle must lose its energy in many such interactions during its passage through an absorber. At any given time, the particle is interacting with many electrons, so the net effect is to decrease its velocity continuously until the particle is stopped.

Representative paths taken by heavy charged particles in their slowing down process are schematically represented in the sketch below. Except at their very end, the tracks tend to be quite straight because the particle is not greatly deflected by any one encounter, and interactions occur in all directions simultaneously. Charged particles are therefore characterized by a definite *range* in a given absorber material. The range, to be defined more precisely below, represents a distance beyond which no particles will penetrate.

The products of these encounters in the absorber are either excited atoms or *ion pairs*. Each ion pair is made up of a free electron and the corresponding positive ion of an absorber atom from which an electron has been totally removed. The ion pairs have a natural tendency to recombine to form neutral atoms, but in some types of detectors, this recombination is suppressed so that the ion pairs may be used as the basis of the detector response.

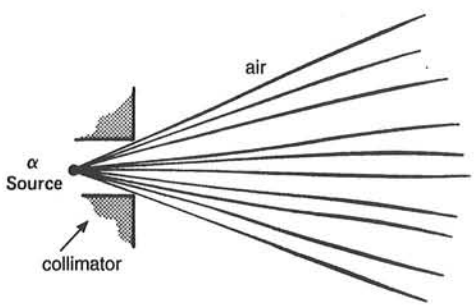

In particularly close encounters, an electron may undergo a large enough impulse that after having left its parent atom, it still may have sufficient kinetic energy to create further ions. These energetic electrons are sometimes called *delta rays* and represent an indirect means by which the charged particle energy is transferred to the absorbing medium. Under typical conditions, the majority of the energy loss of the charged particle occurs via these delta rays. The range of the delta rays is always small compared with the range of the incident energetic particle, so the ionization is still formed close to the primary track. On a microscopic scale, one effect of this process is that the ion pairs normally do not appear as randomly spaced single ionizations, but there is a tendency to form many "clusters" of multiple ion pairs distributed along the track of the particle.

B. Stopping Power

The *linear stopping power S* for charged particles in a given absorber is simply defined as the differential energy loss for that particle within the material divided by the corresponding differential path length:

$$S = -\frac{dE}{dx} \tag{2.1}$$

The value of $-dE/dx$ along a particle track is also called its *specific energy loss* or, more casually, its "rate"of energy loss.

For particles with a given charge state, S increases as the particle velocity is decreased. The classical expression that describes the specific energy loss is known as the *Bethe formula* and is written

$$-\frac{dE}{dx} = \frac{4\pi e^4 z^2}{m_0 v^2} NB \tag{2.2}$$

where

$$B \equiv Z\left[\ln\frac{2m_0v^2}{I} - \ln\left(1-\frac{v^2}{c^2}\right) - \frac{v^2}{c^2}\right]$$

In these expressions, v and ze are the velocity and charge of the primary particle, N and Z are the number density and atomic number of the absorber atoms, m_0 is the electron rest mass, and e is the electronic charge. The parameter I represents the average excitation and ionization potential of the absorber and is normally treated as an experimentally determined parameter for each element. For nonrelativistic charged particles ($v \ll c$), only the first term in B is significant. Equation (2.2) is generally valid for different types of charged particles provided their velocity remains large compared with the velocities of the orbital electrons in the absorbing atoms.

The expression for B in Eq. (2.2) varies slowly with particle energy. Thus, the general behavior of dE/dx can be inferred from the behavior of the multiplicative factor. For a given nonrelativistic particle, dE/dx therefore varies as $1/v^2$, or inversely with particle energy. This behavior can be heuristically explained by noting that because the charged particle spends a greater time in the vicinity of any given electron when its velocity is low, the impulse felt by the electron, and hence the energy transfer, is largest. When comparing different charged particles of the same velocity, the only factor that may change outside the logarithmic term in Eq. (2.2) is z^2, which occurs in the numerator of the expression. Therefore, particles with the greatest charge will have the largest specific energy loss. Alpha particles, for example, will lose energy at a rate that is greater than protons of the same velocity but less than that of more highly charged ions. In comparing different materials as absorbers, dE/dx depends primarily on the product NZ, which is outside the logarithmic term. This product NZ represents

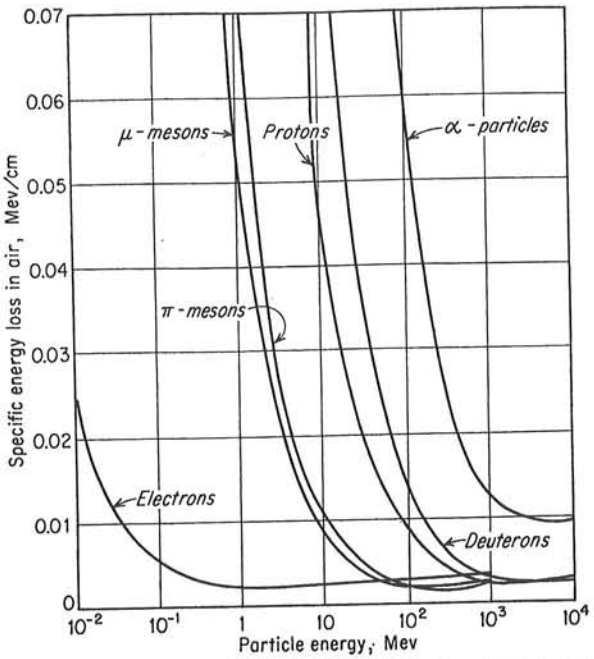

Figure 2.1 Variation of the specific energy loss in air versus energy of the charged particles shown. (From Beiser.[2])

the electron density of the absorber. High atomic number, high-density materials will consequently result in the greatest linear stopping power.

The variation of the specific energy loss for a number of different charged particles is shown in Fig. 2.1 over a wide energy range. This figure shows that the value of dE/dx for many different types of charged particles approaches a near-constant broad minimum value at energies above several hundred MeV, where their velocity approaches the velocity of light. This specific energy loss corresponds to about 2 MeV per g/cm^2 in light materials. Because of their similar energy loss behavior, such relativistic particles are sometimes referred to as "minimum ionizing particles." Fast electrons also fall into this category at energies as low as about 1 MeV because their much lower mass results in relativistic velocities even at such modest energy.

The Bethe formula begins to fail at low particle energies where charge exchange between the particle and absorber becomes important. The positively charged particle will then tend to pick up electrons from the absorber, which effectively reduce its charge and consequent linear energy loss. At the end of its track, the particle has accumulated z electrons and becomes a neutral atom.

C. Energy Loss Characteristics

1. THE BRAGG CURVE

A plot of the specific energy loss along the track of a charged particle such as that shown in Fig. 2.2 is known as a *Bragg curve*. The example is shown for an alpha particle of several MeV initial energy. For most of the track, the charge on the alpha particle is two electronic charges, and the specific energy loss increases roughly as $1/E$ as predicted by Eq. (2.2). Near the end of the track, the charge is reduced through electron pickup and the curve falls off. Plots are shown both for a single alpha particle track and for the average behavior of a parallel beam of alpha particles of the same initial energy. The two curves differ somewhat due to the effects of straggling, to be discussed below.

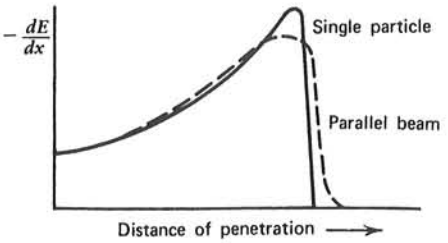

Figure 2.2 The specific energy loss along an alpha track.

Related plots showing $-dE/dx$ versus particle energy for a number of different heavy charged particles are given in Fig. 2.3. These examples illustrate the energy at which charge pickup by the ion becomes significant. Charged particles with the greatest number of nuclear charges begin to pick up electrons early in their slowing-down process. Note that in an aluminum absorber, singly charged hydrogen ions (protons) show strong effects of charge pickup below about 100 keV, but doubly charged ^{3}He ions show equivalent effects at about 400 keV.

2. ENERGY STRAGGLING

Because the details of the microscopic interactions undergone by any specific particle vary somewhat randomly, its energy loss is a statistical or stochastic process. Therefore, a spread in energies always results after a beam of monoenergetic charged particles has passed through a given thickness of absorber. The width of this energy distribution is a measure of energy straggling, which varies with the distance along the particle track.

Figure 2.4 shows a schematic presentation of the energy distribution of a beam of initially monoenergetic particles at various points along its range. Over the first portion, the distribution becomes wider (and more skewed) with penetration distance, showing the

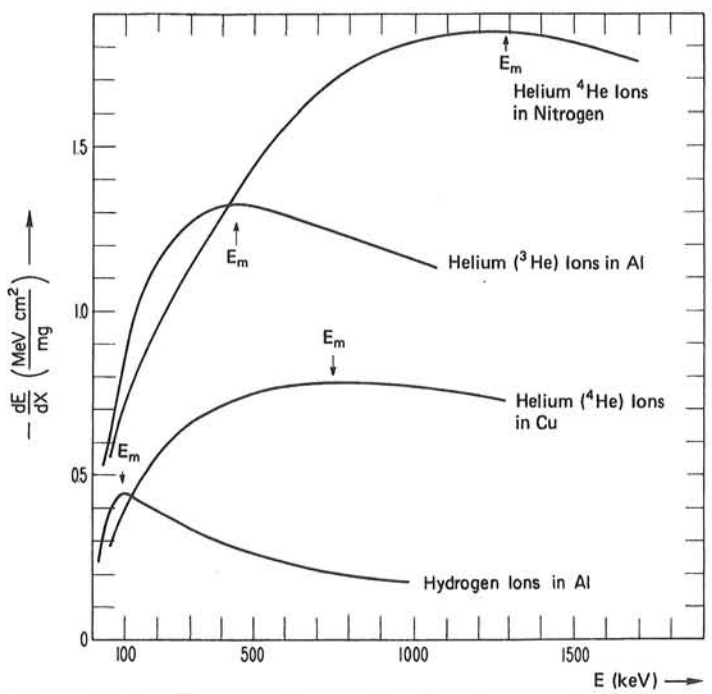

Figure 2.3 Specific energy loss as a function of energy for hydrogen and helium ions. E_m indicates the energy at which dE/dx is maximized. (From Wilken and Fritz.[3])

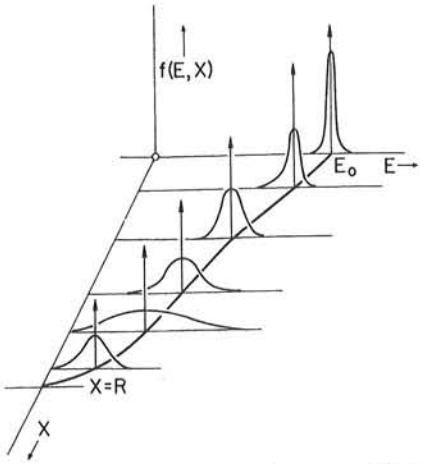

Figure 2.4 Plots of energy distribution of a beam of initially monoenergetic charged particles at various penetration distances. E is the particle energy and X is the distance along the track. (From Wilken and Fritz.[3])

increasing importance of energy straggling. Near the end of the range, the distribution narrows again because the mean particle energy has greatly been reduced.

D. Particle Range

1. DEFINITIONS OF RANGE

In order to quantify the definition of particle range, we refer to the conceptual experiment sketched in Fig. 2.5. Here a collimated source of monoenergetic alpha particles is counted by a detector after passing through an absorber of variable thickness. (We later contrast the behavior of other types of radiation when observed under similar conditions.) For alpha particles, the results are also plotted in Fig. 2.5. For small values of the absorber thickness, the only effect is to cause an energy loss of the alpha particles in the absorber as they pass through. Because the tracks through the absorber are quite straight, the total number that reach the detector remains the same. No attenuation in the number of alpha particles takes place until the absorber thickness approaches the length of the shortest track in the absorbing material. Increasing the thickness then stops more and more of the alpha particles, and the intensity of the detected beam drops rapidly to zero.

The range of the alpha particles in the absorber material can be determined from this curve in several ways. The *mean range* is defined as the absorber thickness that reduces the alpha particle count to exactly one-half of its value in the absence of the absorber.

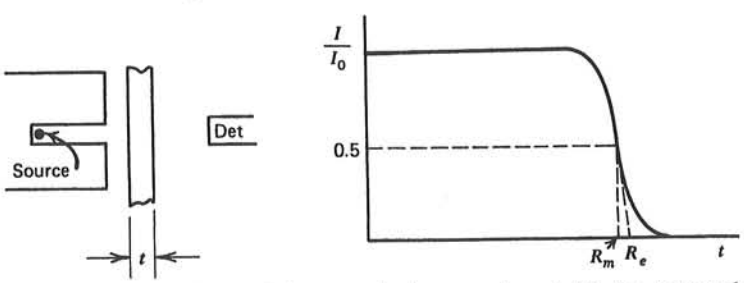

Figure 2.5 An alpha particle transmission experiment. I is the detected number of alpha particles through an absorber thickness t, whereas I_0 is the number detected without the absorber. The mean range R_m and extrapolated range R_e are indicated.

This definition is most commonly used in tables of numerical range values. Another version that appears in the literature is the *extrapolated range*, which is obtained by extrapolating the linear portion of the end of the transmission curve to zero.

The range of charged particles of a given energy is thus a fairly unique quantity in a specific absorber material. In the early days of radiation measurement, experiments of the type sketched in Fig. 2.5 were widely used to measure the energy of alpha particles indirectly by determining the absorber thickness equivalent to their mean range. With the availability of detectors that provide an output signal directly related to the alpha particle energy, such indirect measurements are no longer necessary.

Some graphs of the mean range of various charged particles in materials of interest in detectors are given in Figs. 2.6 through 2.8. As one obvious application of these curves, any detector that is to measure the full incident energy of a charged particle must have an active thickness that is greater than the range of that particle in the detector material.

2. RANGE STRAGGLING

Charged particles are also subject to *range straggling*, defined as the fluctuation in path length for individual particles of the same initial energy. The same stochastic factors that lead to energy straggling at a given penetration distance also result in slightly different

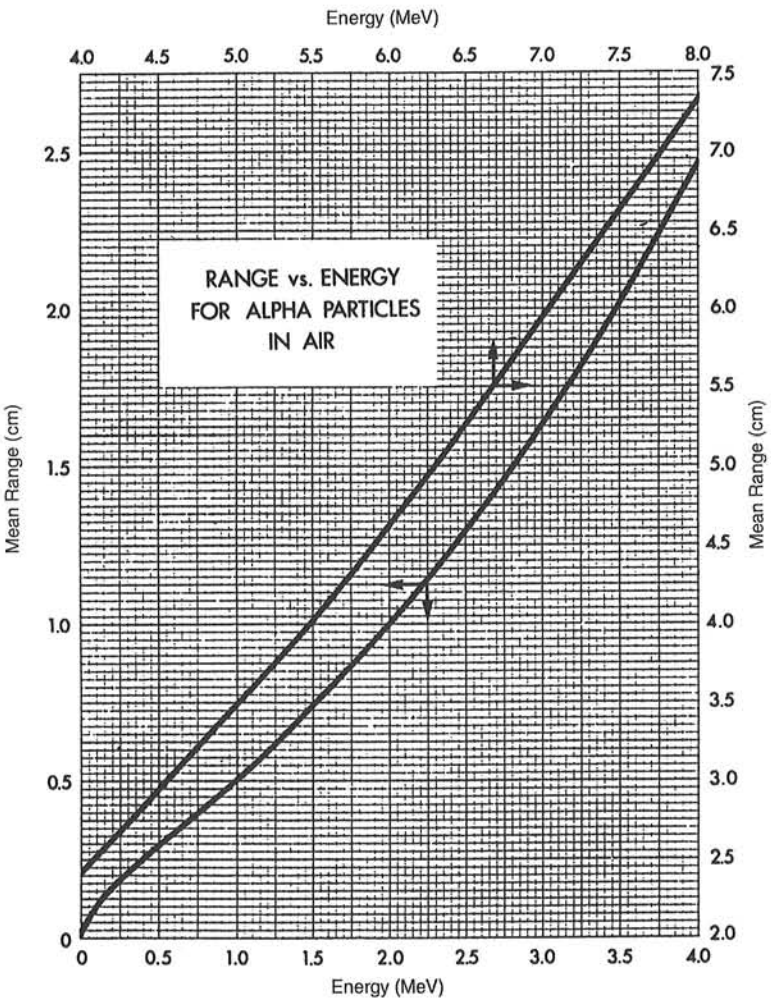

Figure 2.6 Range–energy plot for alpha particles in air at 15°C and 760 mm Hg pressure. (From *Radiological Health Handbook*, U.S. Department of Health, Education and Welfare, Washington, DC, 1970.)

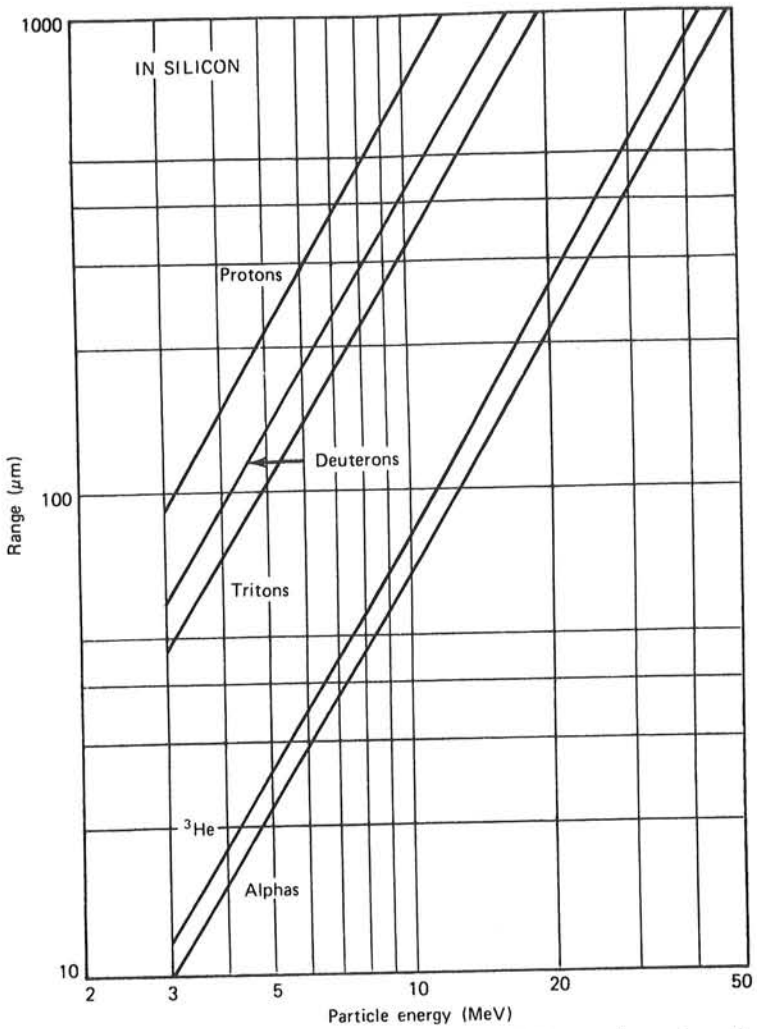

Figure 2.7 Range–energy curves calculated for different charged particles in silicon. The near-linear behavior of the log–log plot over the energy range shown suggests an empirical relation to the form $R = aE^b$, where the slope-related parameter b is not greatly different for the various particles. (From Skyrme.[4])

total path lengths for each particle. For heavy charged particles such as protons or alphas, the straggling amounts to a few percent of the mean range. The degree of straggling is evidenced by the sharpness of the cutoff at the end of the average transmission curve plotted in Fig. 2.2. Differentiating this curve leads to a peak whose width is often taken as a quantitative measure of the importance of range straggling for the particles and absorber used in the measurement.

3. STOPPING TIME

The time required to stop a charged particle in an absorber can be deduced from its range and average velocity. For nonrelativistic particles of mass m and kinetic energy E, the velocity is

$$v = \sqrt{\frac{2E}{m}} = c\sqrt{\frac{2E}{mc^2}} = \left(3.00 \times 10^8 \frac{\text{m}}{\text{s}}\right)\sqrt{\frac{2E}{(931\ \text{MeV/amu})m_A}}$$

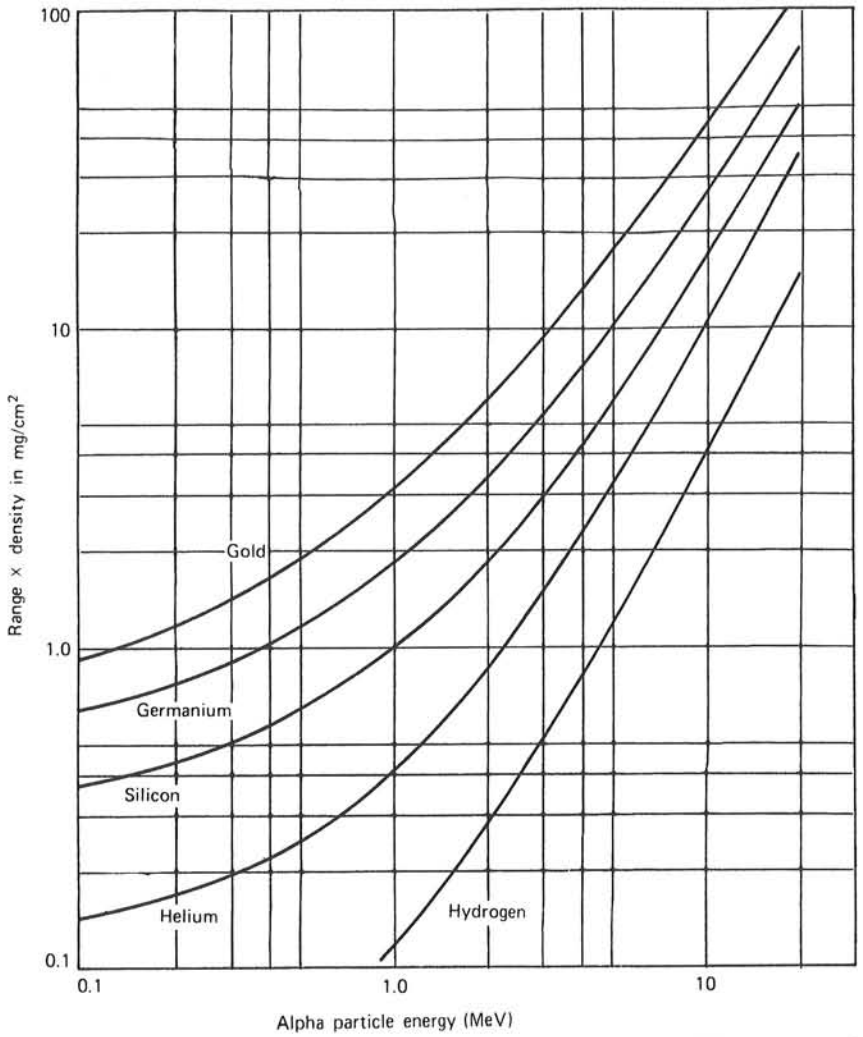

Figure 2.8 Range–energy curves calculated for alpha particles in different materials. Units of the range are given in mass thickness (see p. 54) to minimize the differences in these curves. (Data from Williamson et al.[5])

where m_A is the particle mass in atomic mass units and E is the particle energy in MeV. If we assume that the average particle velocity as it slows down is $\langle v \rangle = Kv$, where v is evaluated at the initial energy, then the stopping time T can be calculated from the range R as

$$T = \frac{R}{\langle v \rangle} = \frac{R}{Kc}\sqrt{\frac{mc^2}{2E}} = \frac{R}{K(3.00 \times 10^8 \text{ m/s})}\sqrt{\frac{931 \text{ MeV/amu}}{2}}\sqrt{\frac{m_A}{E}}$$

If the particle were uniformly decelerated, then $\langle v \rangle$ would be given by $v/2$ and K would be 0.5. However, charged particles generally lose energy at a greater rate near the end of their range, and K should be a somewhat higher fraction. By assuming $K = 0.60$, the stopping time can be estimated as

$$T \cong 1.2 \times 10^{-7} R \sqrt{\frac{m_A}{E}} \tag{2.3}$$

where T is in seconds, R in meters, m_A in amu, and E in MeV. This approximation is expected to be reasonably accurate for light charged particles (protons, alpha particles, etc.) over much of the energy range of interest here. It is not, however, to be used for relativistic particles such as fast electrons.

Using typical range values, stopping times calculated from Eq. (2.3) for charged particles are a few picoseconds in solids or liquids and a few nanoseconds in gases. These times are generally small enough to be neglected for all but the fastest-responding radiation detectors.

E. Energy Loss in Thin Absorbers

For thin absorbers (or detectors) that are penetrated by a given charged particle, the energy deposited within the absorber can be calculated from

$$\Delta E = -\left(\frac{dE}{dx}\right)_{\text{avg}} t \tag{2.4}$$

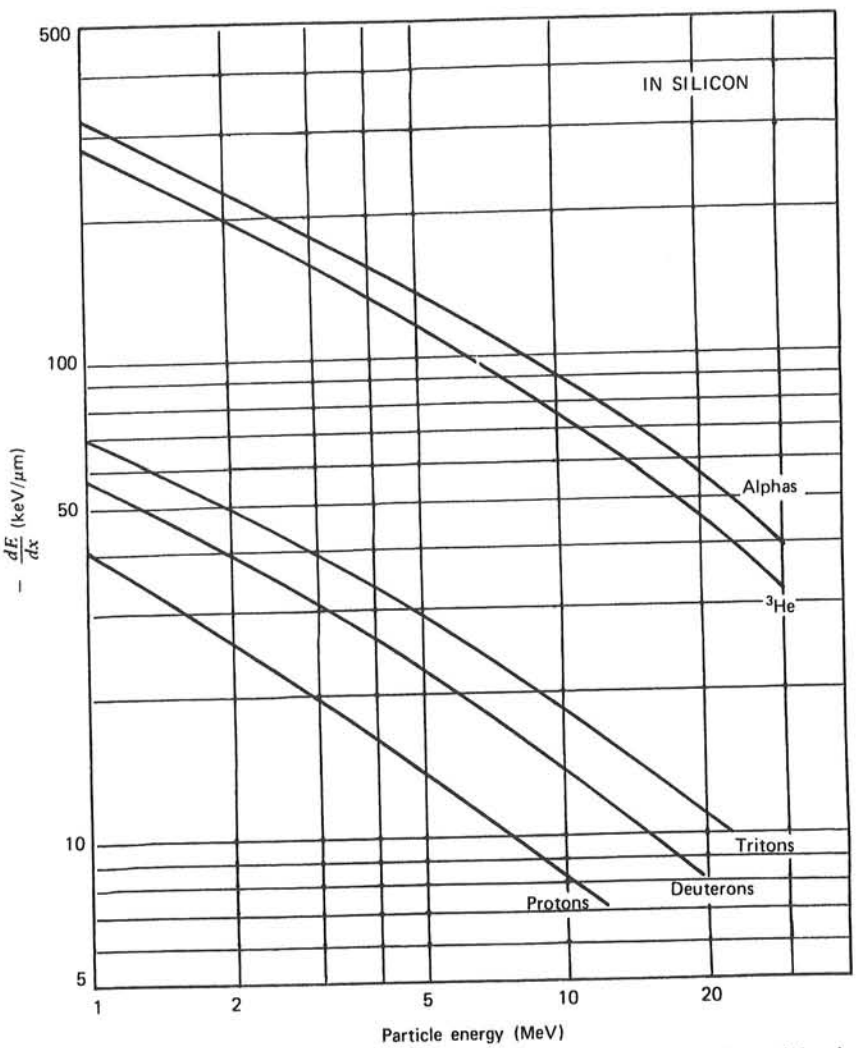

Figure 2.9 The specific energy loss calculated for different charged particles in silicon. (From Skyrme.[4])

where t is the absorber thickness and $(-dE/dx)_{avg}$ is the linear stopping power averaged over the energy of the particle while in the absorber. If the energy loss is small, the stopping power does not change much and it can be approximated by its value at the incident particle energy. Tabular values for dE/dx for a number of different charged particles in a variety of absorbing media are given in Refs. 5–10. Some graphs for materials of interest are shown in Figs. 2.9 through 2.11.

For absorber thicknesses through which the energy loss is not small, it is not simple to obtain a properly weighted $(-dE/dx)_{avg}$ value directly from such data. In these cases, it is easier to obtain the deposited energy in a way that makes use of range–energy data of the type plotted in Figs. 2.6 through 2.8. The basis of the method is as follows: Let R_1 represent the full range of the incident particle with energy E_0 in the absorber material. By subtracting the physical thickness of the absorber t from R_1, a value R_2 is obtained that represents the range of those alpha particles that emerge from the opposite surface of the absorber. By finding the energy corresponding to R_2, the energy of the transmitted charged particles

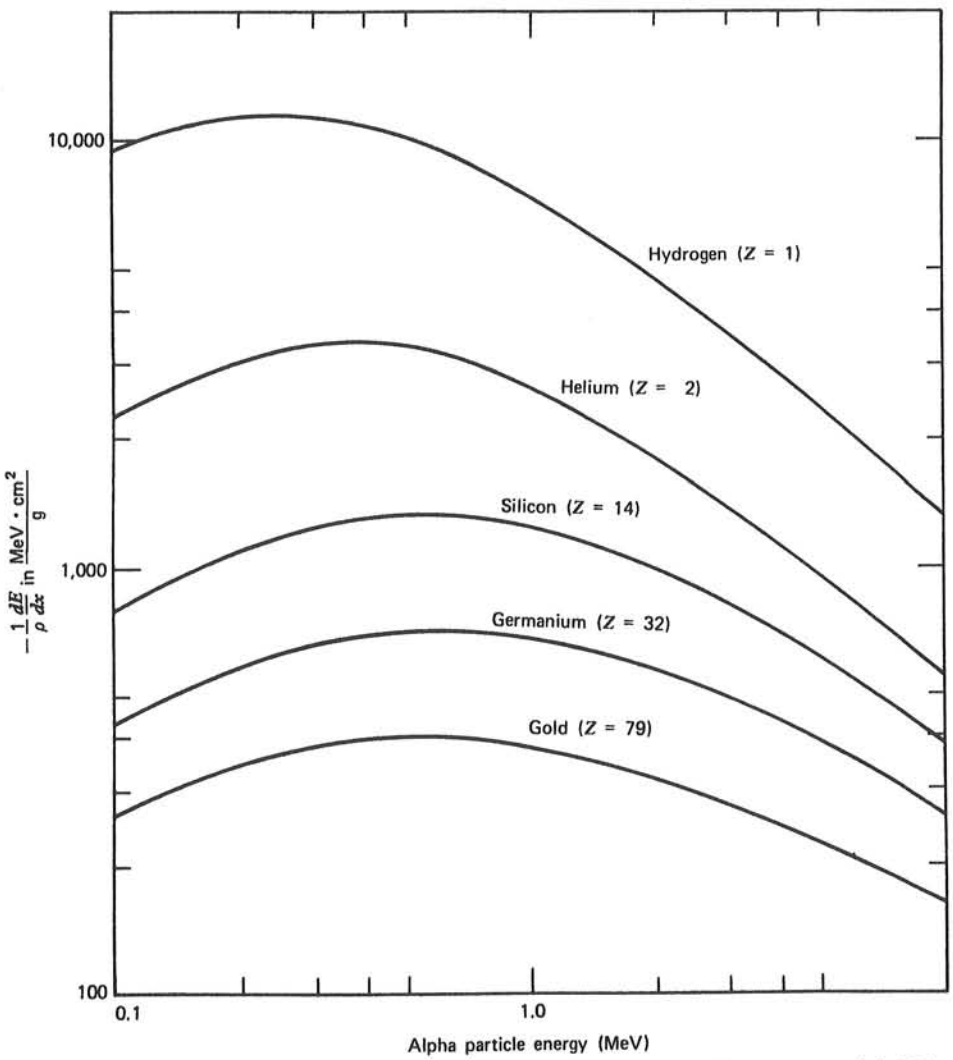

Figure 2.10 The specific energy loss calculated for alpha particles in different materials. Values are normalized by the density of the absorber material. (Data from Williamson et al.[5])

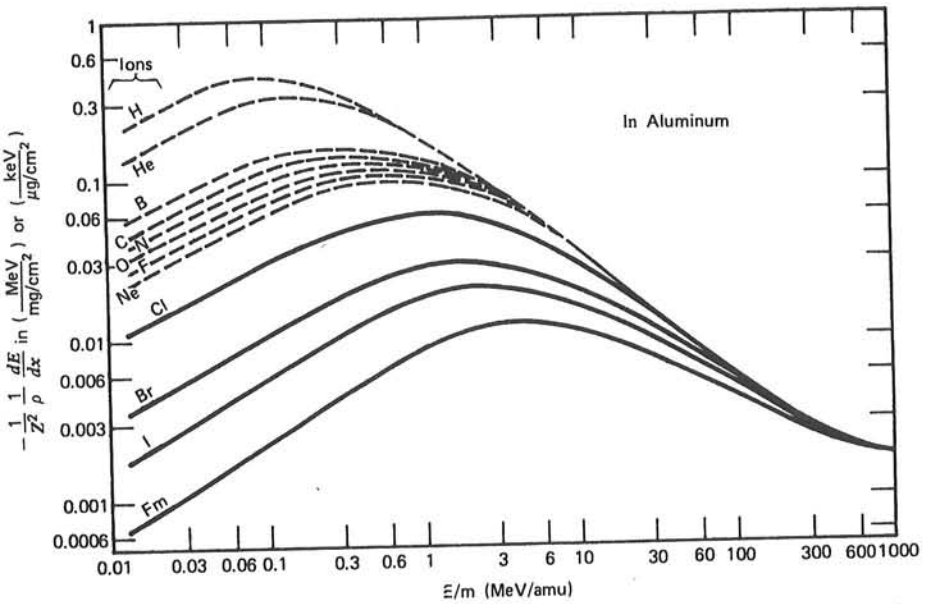

Figure 2.11 Plots showing the specific energy loss of various heavy ions in aluminum. The abscissa is the ion energy divided by its mass, and the ordinate is $-dE/dx$ divided by the density of aluminum and the square of the ion atomic number. Typical fission fragments (e.g., iodine) show a continuously decreasing $-dE/dx$ while slowing from their initial energy (~1 MeV/amu). (From Northcliffe and Schilling.[8])

E_t is obtained. The deposited energy ΔE is then given simply by $E_0 - E_t$. These steps are illustrated below:

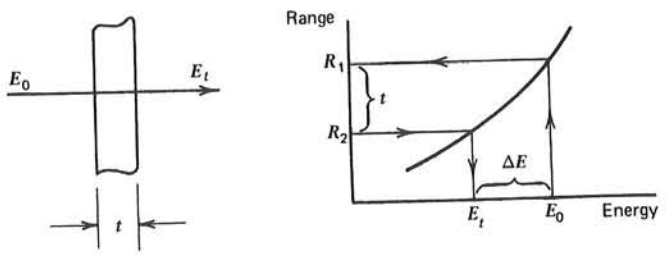

The procedure is based on the assumption that the charged particle tracks are perfectly linear in the absorber, and the method does not apply in situations where the particle can be significantly deflected (such as for fast electrons).

The combined effects of particle range and the decrease in dE/dx with increasing energy are illustrated in Fig. 2.12. Here the energy loss of protons in a thin detector is plotted versus the incident proton energy. For low energies, the proton range is less than the detector thickness. Therefore, as the energy is increased, the energy deposited in the detector (which is just equal to the incident energy) increases linearly. At a proton energy of 425 keV, the range is exactly equal to the detector thickness. For higher energies, only a portion of incident energy is deposited, and the transmitted proton carries off the remainder. Under these conditions, the energy deposited in the detector is given by Eq. (2.4), or simply the product of the detector thickness and the average linear stopping power. Because the stopping power continuously decreases with increasing energy in this region (see Fig. 2.3), the deposited energy therefore *decreases* with further increases in the

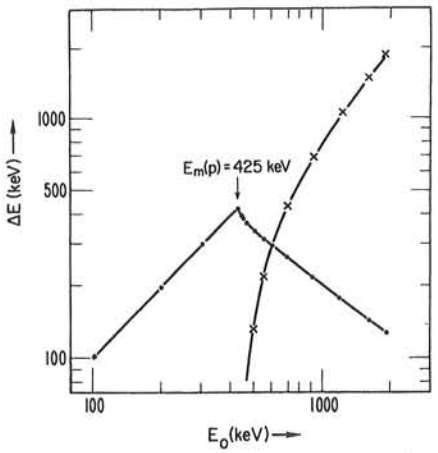

Figure 2.12 Energy loss of protons of initial energy E_0 in a silicon detector of 4.6 μm thickness (shown as dots). The transmitted energy for penetrating protons is also shown (as crosses). (From Wilken and Fritz.[3])

incident proton energy. The second curve in Fig. 2.12 plots the transmitted energy (E_t on the diagram on the preceding page) as recorded by a second thick detector.

F. Scaling Laws

Sometimes data are not available on the range or energy loss characteristics of precisely the same particle-absorber combination needed in a given experiment. Recourse must then be made to various approximations, most of which are derived based on the Bethe formula [Eq. (2.2)] and on the assumption that the stopping power per atom of compounds or mixtures is additive. This latter assumption, known as the *Bragg–Kleeman rule*, may be written

$$\frac{1}{N_c}\left(\frac{dE}{dx}\right)_c = \sum_i W_i \frac{1}{N_i}\left(\frac{dE}{dx}\right)_i \tag{2.5}$$

In this expression, N is the atomic density, dE/dx is the linear stopping power, and W_i represents the atom fraction of the ith component in the compound (subscript c). As an example of the application of Eq. (2.5), the linear stopping power of alpha particles in a metallic oxide could be obtained from separate data on the stopping power in both the pure metal and in oxygen. Some caution should be used in applying such results, however, since some measurements[12–15] for compounds have indicated a stopping power differing by as much as 10–20% from that calculated from Eq. (2.5).

It can be shown[11] that the range of a charged particle in a compound material can also be estimated provided its range is known in all the constituent elements. In this derivation, it is necessary to assume that the shape of the dE/dx curve is independent of the stopping medium. Under these conditions, the range in the compound is given by

$$R_c = \frac{M_c}{\sum_i n_i (A_i/R_i)} \tag{2.6}$$

where R_i is the range in element i, n_i is the number of atoms of element i in the molecule, A_i is the atomic weight of element i, and M_c is the molecular weight of the compound.

If range data are not available for all the constituent elements, estimates can be made based on a semiempirical formula (commonly called the Bragg–Kleeman rule as well)

$$\frac{R_1}{R_0} \cong \frac{\rho_0\sqrt{A_1}}{\rho_1\sqrt{A_0}} \tag{2.7}$$

where ρ and A represent density and atomic weight, and subscripts 0 and 1 refer to different absorbing materials. The accuracy of this estimate diminishes when the two materials are of widely different atomic weights, so it is always best to use range data from a material that is as close as possible in A to the absorber of interest.

Range data can also be generalized to different charged particles within a given absorber material. By integration of Eq. (2.2), it can be shown that the range of a particle of mass m and charge z can be represented by

$$R(v) = \frac{m}{z^2} F(v) \tag{2.8}$$

where $F(v)$ represents a unique function of the particle initial velocity v. For particles of the same initial velocity, this factor will be identical and therefore we can write

$$R_a(v) = \frac{m_a z_b^{\,2}}{m_b z_a^{\,2}} R_b(v) \tag{2.9}$$

where the subscripts a and b refer to different charged particles. Thus, the range of a particle for which data are not available can be estimated by calculating its initial velocity, finding the range of any other particle of the same initial velocity in the same material, and applying Eq. (2.9). It should be emphasized that these estimates are only approximate, because no account is taken of the change in charge state of the particle as it nears the end of its path. Correction factors necessary to compensate for this effect and predict the range more accurately are presented by Evans.[1]

G. Behavior of Fission Fragments

The heavy fragments produced as a result of neutron-induced or spontaneous fission of heavy nuclei are energetic charged particles with properties somewhat different from those discussed up to this point. Because the fragments start out stripped of many electrons, their very large effective charge results in a specific energy loss greater than that encountered with any other radiations discussed in this text. Because the initial energy is also very high (see Fig. 1.4*b*), however, the range of a typical fission fragment is approximately half that of a 5 MeV alpha particle.

An important feature of a fission fragment track is the fact that the specific energy loss $(-dE/dx)$ decreases as the particle loses energy in the absorber. This behavior is in marked contrast to the lighter particles, such as alpha particles or protons, and is a result of the continuous decrease in the effective charge carried by the fragment as its velocity is reduced. The pickup of electrons begins immediately at the start of the track, and therefore the factor z in the numerator of Eq. (2.2) continuously drops. The resulting decrease in $-dE/dx$ is large enough to overcome the increase that normally accompanies a reduction in velocity. For particles with much lower initial charge state, such as the alpha particle, electron pickup does not become significant until near the end of the range.

H. Secondary Electron Emission from Surfaces

As charged particles lose their kinetic energy during the slowing-down process, many electrons from the absorber are given a sufficient impulse to travel a short distance from the original track of the particle. These include the delta rays mentioned earlier, whose energy is high enough to ionize other absorber atoms, and also electrons whose kinetic energy of only a few eV is below the minimum energy for further ionization. If an energetic charged

particle is incident on or emerges from a solid surface, some of these electrons may migrate to the surface and have sufficient energy to escape. The term *secondary electrons* is conventionally applied to these escaping low-energy electrons. (*Note*: The same term is often used to characterize the much more energetic electrons formed in the gamma-ray interactions described later in this chapter—a very different type of secondary electron.)

A single heavy ion such as a fission fragment can produce hundreds of these escaping secondaries, whereas lighter alpha particles might typically result in 10 or fewer secondaries per particle.[16] Fast electrons such as beta particles are much less likely to create escaping secondaries, and only a few percent will result in secondary emission. To a first approximation, the yield of secondaries will be proportional to the energy lost within a near-surface layer whose thickness represents the maximum distance an electron will tend to migrate from its point of origin and still retain enough energy to escape from the surface. Thus, the dE/dx value of the particle is a reasonable predictor of secondary yield from a given material. Those materials with low work function and large escape distance will have the largest yield. Thin films of alkali halides, and cesium iodide in particular, are observed to produce secondaries with high yield. Models of the electron transport in alkali halides[17] confirm their suitability as prolific sources of secondary electrons.

The energy spectrum of these escaping secondary electrons is a continuum with a mean value that is very low compared with the primary particle energy. For example, the energy of secondaries from a carbon surface average 60–100 eV for alpha particles and 290 eV for fission fragments.[16] The energy of secondary electrons produced by lighter particles such as fast electrons is even lower. Thus it is normally difficult or impossible to observe the secondaries since they are readily reabsorbed even in air. If they are emitted into a vacuum or low-pressure gas, however, they can be accelerated and easily guided by electric fields because of their low initial velocity. For example, an electric field created by the application of 1000 V with respect to the surface would have a strong influence on the trajectory of a 100 eV electron, but almost no effect on a 1 MeV fast electron. This property has led to the successful use of secondary electron emission from surfaces as a means of detecting the positions at which beta particles emerge from a surface[18] and in the imaging of X-rays and fast electrons.[19] Secondary electrons emitted from a thin foil and directed to an external electron detector such as a microchannel plate have also served as the basis for fast timing measurements with heavy ions.[20,21] One special application of the secondary electron emission process will be detailed in Chapter 9, where a typical electron in a photomultiplier tube is accelerated to a few hundred eV before striking a solid surface, causing the emission of 5–10 secondaries in a charge multiplication process.

II. INTERACTION OF FAST ELECTRONS

When compared with heavy charged particles, fast electrons lose their energy at a lower rate and follow a much more tortuous path through absorbing materials. A series of tracks from a source of monoenergetic electrons might appear as in the sketch below:

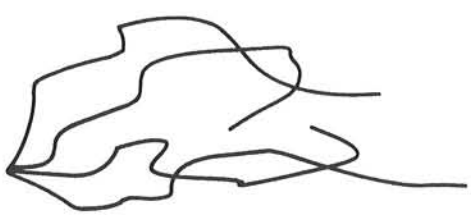

Large deviations in the electron path are now possible because its mass is equal to that of the orbital electrons with which it is interacting, and a much larger fraction of its energy can be lost in a single encounter. In addition, electron–nuclear interactions, which can abruptly change the electron direction, sometimes occur.

A. Specific Energy Loss

An expression similar to that of Eq. (2.2) has also been derived by Bethe to describe the specific energy loss due to ionization and excitation (the " collisional losses") for fast electrons:

$$-\left(\frac{dE}{dx}\right)_c = \frac{2\pi e^4 NZ}{m_0 v^2}\left(\ln\frac{m_0 v^2 E}{2I^2(1-\beta^2)} - (\ln 2)(2\sqrt{1-\beta^2} - 1 + \beta^2) + (1-\beta^2) + \frac{1}{8}\left(1-\sqrt{1-\beta^2}\right)^2\right) \quad (2.10)$$

where the symbols have the same meaning as in Eq. (2.2) and $\beta \equiv v/c$.

Electrons also differ from heavy charged particles in that energy may be lost by radiative processes as well as by coulomb interactions. These radiative losses take the form of *bremsstrahlung* or electromagnetic radiation, which can emanate from any position along the electron track. From classical theory, any charge must radiate energy when accelerated, and the deflections of the electron in its interactions with the absorber correspond to such acceleration. The linear specific energy loss through this radiative process is

$$-\left(\frac{dE}{dx}\right)_r = \frac{NEZ(Z+1)e^4}{137 m_0^2 c^4}\left(4\ln\frac{2E}{m_0c^2} - \frac{4}{3}\right) \quad (2.11)$$

For the particle types and energy ranges of interest in this text, only fast electrons can have a significant yield of bremsstrahlung. The yield from heavy charged particles is negligible as indicated by the presence of the m_0^2 factor in the denominator of the multiplicative term in Eq. (2.11). The factors of E and Z^2 in the numerator of Eq. (2.11) show that radiative losses are most important for high electron energies and for absorber materials of large atomic number. For typical electron energies, the average bremsstrahlung photon energy is quite low (see Fig. 1.6) and is therefore normally reabsorbed fairly close to its point of origin. In some cases, however, the escape of bremsstrahlung can influence the response of small detectors.

The total linear stopping power for electrons is the sum of the collisional and radiative losses:

$$\frac{dE}{dx} = \left(\frac{dE}{dx}\right)_c + \left(\frac{dE}{dx}\right)_r \quad (2.12)$$

The ratio of the specific energy losses is given approximately by

$$\frac{(dE/dx)_r}{(dE/dx)_c} \cong \frac{EZ}{700} \quad (2.13)$$

where E is in units of MeV. For the electrons of interest here (such as beta particles or secondary electrons from gamma-ray interactions), typical energies are less than a few MeV. Therefore, radiative losses are always a small fraction of the energy losses due to ionization and excitation and are significant only in absorber materials of high atomic number.

B. Electron Range and Transmission Curves

1. ABSORPTION OF MONOENERGETIC ELECTRONS

An attenuation experiment of the type discussed earlier for alpha particles is sketched in Fig. 2.13 for a source of monoenergetic fast electrons. Even small values of the absorber thickness lead to the loss of some electrons from the detected beam because scattering of the electron effectively removes it from the flux striking the detector. A plot of the detected number of electrons versus absorber thickness therefore begins to drop immediately and gradually approaches zero for large absorber thicknesses. Those electrons that penetrate

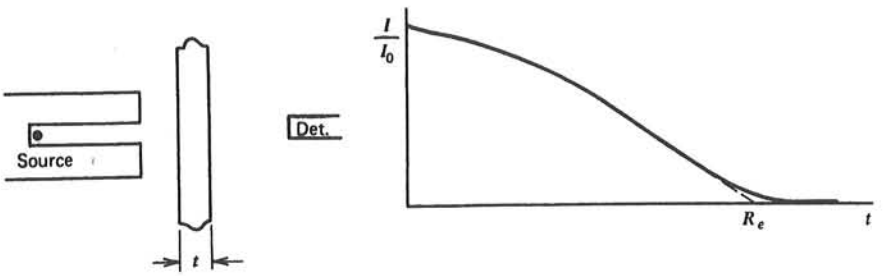

Figure 2.13 Transmission curve for monoenergetic electrons. R_e is the extrapolated range.

the greatest absorber thickness will be the ones whose initial direction has changed least in their path through the absorber.

The concept of range is less definite for fast electrons than for heavy charged particles, because the electron total path length is considerably greater than the distance of penetration along the initial velocity vector. Normally, the electron range is taken from a transmission plot, such as that given in Fig. 2.13, by extrapolation of the linear portion of the

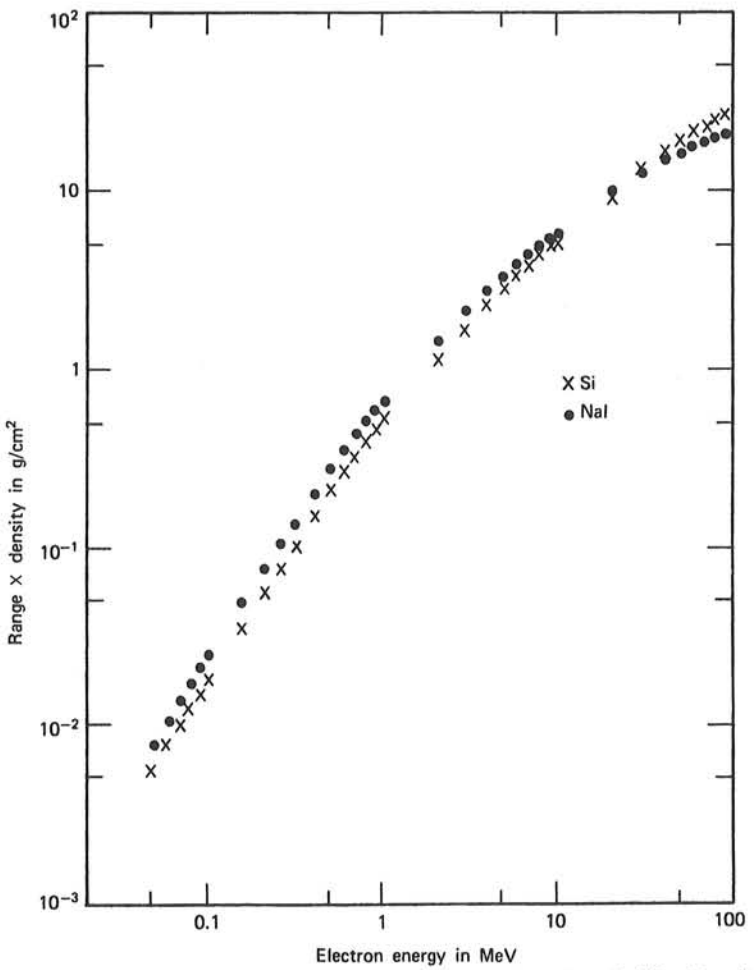

Figure 2.14 Range–energy plots for electrons in silicon and sodium iodide. If units of mass thickness (distance × density) are used for the range as shown, values at the same electron energy are similar even for materials with widely different physical properties or atomic number. (Data from Mukoyama.[24])

curve to zero and represents the absorber thickness required to ensure that almost no electrons can penetrate the entire thickness.

For equivalent energy, the specific energy loss of electrons is much lower than that of heavy charged particles, so their path length in typical absorbers is hundreds of times greater. As a very crude estimate, electron ranges tend to be about 2 mm per MeV in low-density materials, or about 1 mm per MeV in materials of moderate density.

Tabular data are given in Refs. 22 and 23 for the stopping power and range of electrons and positrons in elements and compounds, covering a large region of energy. To a fair degree of approximation, the product of the range times the density of the absorber is a constant for different materials for electrons of equal initial energy. Plots of the range of electrons in two common detector materials are given in Fig. 2.14.

2. *ABSORPTION OF BETA PARTICLES*

The transmission curve for beta particles emitted by a radioisotope source, because of the continuous distribution in their energy, differs significantly from that sketched in Fig. 2.13 for monoenergetic electrons. The "soft" or low-energy beta particles are rapidly absorbed even in small thicknesses of the absorber, so that the initial slope on the attenuation curve is much greater. For the majority of beta spectra, the curve happens to have a near-exponential shape and is therefore nearly linear on the semilog plot of the type shown in Fig. 2.15. This exponential behavior is only an empirical approximation and does not have a fundamental basis as does the exponential attenuation of gamma rays [see Eq. (2.20)]. An *absorption coefficient* n is sometimes defined by

$$\frac{I}{I_0} = e^{-nt} \tag{2.14}$$

where I_0 = counting rate without absorber

I = counting rate with absorber

t = absorber thickness in g/cm^2

The coefficient n correlates well with the endpoint energy of the beta emitter for a specific absorbing material. This dependence is shown in Fig. 2.16 for aluminum. Through the use of such data, attenuation measurements can be used to identify indirectly endpoint

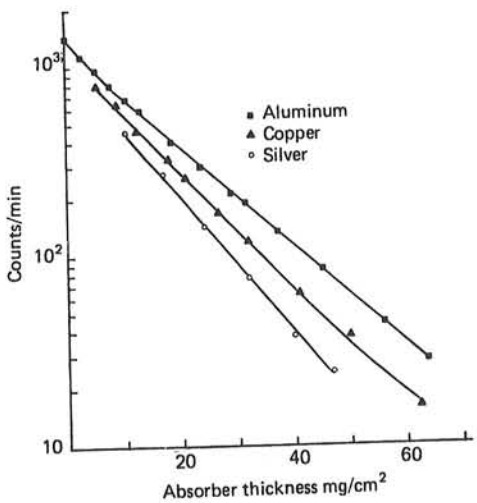

Figure 2.15 Transmission curves for beta particles from ^{185}W (endpoint energy of 0.43 MeV). (From Baltakmens.[25])

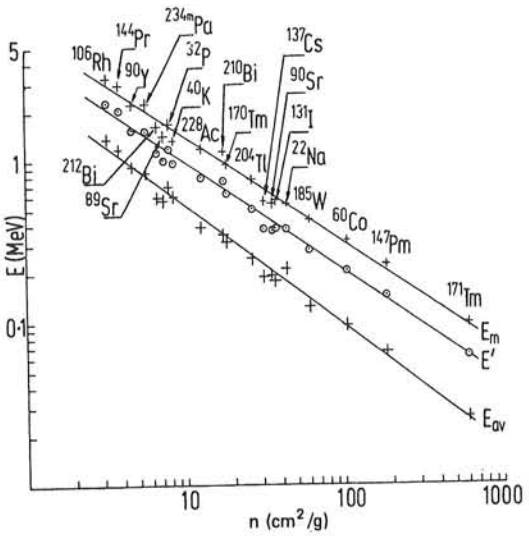

Figure 2.16 Beta particle absorption coefficient n in aluminum as a function of the endpoint energy E_m, average energy E_{av}, and $E' \equiv 0.5\ (E_m + E_{av})$ of different beta emitters. (From Baltakmens.[26])

energies of unknown beta emitters, although direct energy measurements are more common.

3. BACKSCATTERING

The fact that electrons often undergo large-angle deflections along their tracks leads to the phenomenon of *backscattering*. An electron entering one surface of an absorber may undergo sufficient deflection so that it re-emerges from the surface through which it entered. These backscattered electrons do not deposit all their energy in the absorbing medium and therefore can have a significant effect on the response of detectors designed to measure the energy of externally incident electrons. Electrons that backscatter in the detector "entrance window" or dead layer will escape detection entirely.

Backscattering is most pronounced for electrons with low incident energy and absorbers with high atomic number. Figure 2.17 shows the fraction of monoenergetic electrons that are backscattered when normally incident on the surface of various absorbers. Additional data for materials commonly used as electron detectors are given in Table 10.1.

Backscattering can also influence the apparent yield from radioisotope sources of beta particles or conversion electrons. If the source is deposited on a thick backing, electrons that are emitted initially into this backing may backscatter and re-emerge from the surface of the source.

C. Positron Interactions

The coulomb forces that constitute the major mechanism of energy loss for both electrons and heavy charged particles are present for either positive or negative charge on the particle. Whether the interaction involves a repulsive or attractive force between the incident particle and orbital electron, the impulse and energy transfer for particles of equal mass are about the same. Therefore, the tracks of positrons in an absorber are similar to those of normal negative electrons, and their specific energy loss and range are about the same for equal initial energies.

Positrons differ significantly, however, in that the annihilation radiation described in Chapter 1 is generated at the end of the positron track. Because these 0.511 MeV photons are very penetrating compared with the range of the positron, they can lead to the deposition of energy far from the original positron track.

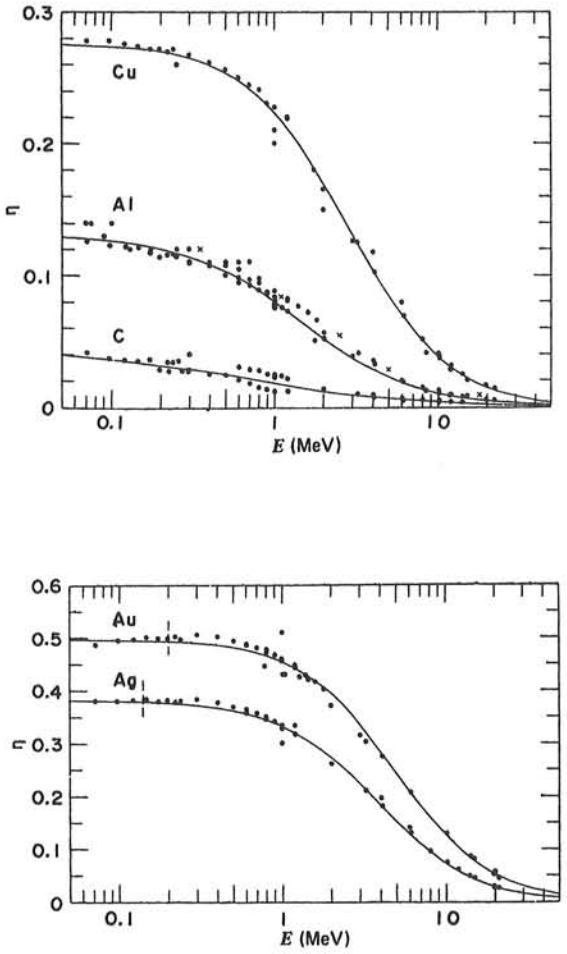

Figure 2.17 Fraction η of normally incident electrons that are backscattered from thick slabs of various materials, as a function of incident energy E. (From Tabata et al.[27])

III. INTERACTION OF GAMMA RAYS

Although a large number of possible interaction mechanisms are known for gamma rays in matter, only three major types play an important role in radiation measurements: *photoelectric absorption, Compton scattering,* and *pair production.* All these processes lead to the partial or complete transfer of the gamma-ray photon energy to electron energy. They result in sudden and abrupt changes in the gamma-ray photon history, in that the photon either disappears entirely or is scattered through a significant angle. This behavior is in marked contrast to the charged particles discussed earlier in this chapter, which slow down gradually through continuous, simultaneous interactions with many absorber atoms. The fundamentals of the gamma-ray interaction mechanisms are introduced here but are again reviewed at the beginning of Chapter 10 in the context of their influence on the response of gamma-ray detectors.

A. Interaction Mechanisms

1. PHOTOELECTRIC ABSORPTION

In the photoelectric absorption process, a photon undergoes an interaction with an absorber atom in which the photon completely disappears. In its place, an energetic *photoelectron* is ejected by the atom from one of its bound shells. The interaction is with the atom as a whole and cannot take place with free electrons. For gamma rays of sufficient energy, the most probable origin of the photoelectron is the most tightly bound or K shell of the atom. The photoelectron appears with an energy given by

$$E_{e-} = h\nu - E_b \tag{2.15}$$

where E_b represents the binding energy of the photoelectron in its original shell. For gamma-ray energies of more than a few hundred keV, the photoelectron carries off the majority of the original photon energy.

In addition to the photoelectron, the interaction also creates an ionized absorber atom with a vacancy in one of its bound shells. This vacancy is quickly filled through capture of a free electron from the medium and/or rearrangement of electrons from other shells of the atom. Therefore, one or more characteristic X-ray photons may also be generated. Although in most cases these X-rays are reabsorbed close to the original site through photoelectric absorption involving less tightly bound shells, their migration and possible escape from radiation detectors can influence their response (see Chapter 10). In some fraction of the cases, the emission of an Auger electron may substitute for the characteristic X-ray in carrying away the atomic excitation energy.

As an example of the complexity of these interactions, consider incident photons with energy above 30 keV that undergo photoelectric absorption in xenon. About 86% interact through K-shell absorptions in the xenon atom.[28] Of these, 87.5% result in K-shell characteristic (or "fluorescent") X-rays (a mixture of K-α and K-β) and 12.5% de-excite through the emission of Auger electrons. The remaining 14% of the incident photons that do not undergo K-shell interactions are absorbed through photoelectric interaction with the L or M shells. These result in much lower energy characteristic X-rays or Auger electrons that are very short range and, to first approximation, are reabsorbed very near the site of the original interaction. Another example of such a "cascade sequence" is shown in Chapter 10 as Fig. 10.20.

The photoelectric process is the predominant mode of interaction for gamma rays (or X-rays) of relatively low energy. The process is also enhanced for absorber materials of high atomic number Z. No single analytic expression is valid for the probability of photoelectric absorption per atom over all ranges of E_γ and Z, but a rough approximation is

$$\tau \cong \text{constant} \times \frac{Z^n}{E_\gamma^{3.5}} \tag{2.16}$$

where the exponent n varies between 4 and 5 over the gamma-ray energy region of interest.[1] This severe dependence of the photoelectric absorption probability on the atomic number of the absorber is a primary reason for the preponderance of high-Z materials (such as lead) in gamma-ray shields. As further detailed in Chapter 10, many detectors used for gamma-ray spectroscopy are chosen from high-Z constituents for the same reason.

A plot of the photoelectric absorption cross section for a popular gamma-ray detection material, sodium iodide, is shown in Fig. 2.18. In the low-energy region, discontinuities in the curve or "absorption edges" appear at gamma-ray energies that correspond to the binding energies of electrons in the various shells of the absorber atom. The edge lying highest in energy therefore corresponds to the binding energy of the K-shell electron. For gamma-ray energies slightly above the edge, the photon energy is just sufficient to undergo a photoelectric interaction in which a K-electron is ejected from the atom. For gamma-ray

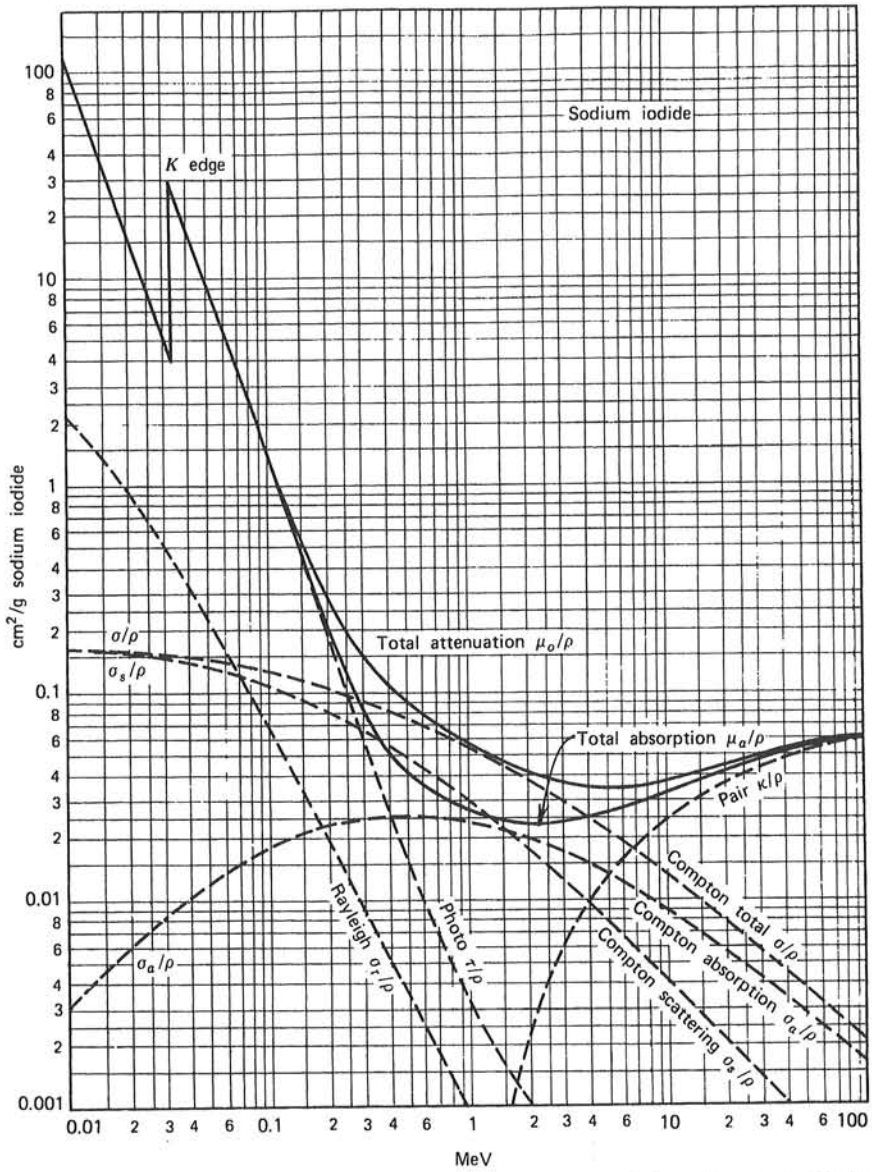

Figure 2.18 Energy dependence of the various gamma–ray interaction processes in sodium iodide. (From *The Atomic Nucleus* by R. D. Evans. Copyright 1955 by the McGraw-Hill Book Company. Used with permission.)

energies slightly below the edge, this process is no longer energetically possible and therefore the interaction probability drops abruptly. Similar absorption edges occur at lower energies for the $L, M, \ldots$ electron shells of the atom.

2. COMPTON SCATTERING

The interaction process of Compton scattering takes place between the incident gamma-ray photon and an electron in the absorbing material. It is most often the predominant interaction mechanism for gamma-ray energies typical of radioisotope sources.

In Compton scattering, the incoming gamma-ray photon is deflected through an angle θ with respect to its original direction. The photon transfers a portion of its energy to the electron (assumed to be initially at rest), which is then known as a *recoil electron*. Because

all angles of scattering are possible, the energy transferred to the electron can vary from zero to a large fraction of the gamma-ray energy.

The expression that relates the energy transfer and the scattering angle for any given interaction can simply be derived by writing simultaneous equations for the conservation of energy and momentum. Using the symbols defined in the sketch below

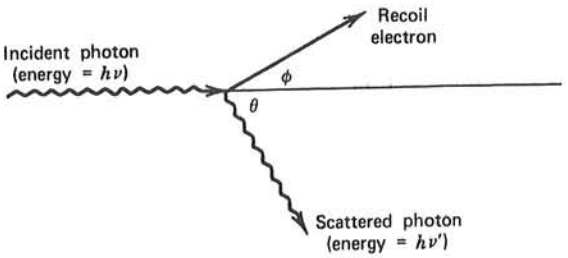

we can show[1] that

$$h\nu' = \frac{h\nu}{1 + \dfrac{h\nu}{m_0c^2}(1 - \cos\theta)} \tag{2.17}$$

where m_0c^2 is the rest-mass energy of the electron (0.511 MeV). For small scattering angles θ, very little energy is transferred. Some of the original energy is always retained by the incident photon, even in the extreme of $\theta = \pi$. Equations (10.3) through (10.6) describe some properties of the energy transfer for limiting cases. A plot of the scattered photon energy predicted from Eq. (2.17) is also shown in Fig. 10.7.†

The probability of Compton scattering per atom of the absorber depends on the number of electrons available as scattering targets and therefore increases linearly with Z. The dependence on gamma-ray energy is illustrated in Fig. 2.18 for the case of sodium iodide and generally falls off gradually with increasing energy.

The angular distribution of scattered gamma rays is predicted by the *Klein–Nishina formula* for the differential scattering cross section $d\sigma/d\Omega$:

$$\frac{d\sigma}{d\Omega} = Zr_0^2\left(\frac{1}{1 + \alpha(1 - \cos\theta)}\right)^2\left(\frac{1 + \cos^2\theta}{2}\right)\left(1 + \frac{\alpha^2(1 - \cos\theta)^2}{(1 + \cos^2\theta)[1 + \alpha(1 - \cos\theta)]}\right) \tag{2.18}$$

where $\alpha \equiv h\nu/m_0c^2$ and r_0 is the classical electron radius. The distribution is shown graphically in Fig. 2.19 and illustrates the strong tendency for forward scattering at high values of the gamma-ray energy.

3. PAIR PRODUCTION

If the gamma-ray energy exceeds twice the rest-mass energy of an electron (1.02 MeV), the process of pair production is energetically possible. As a practical matter, the probability of this interaction remains very low until the gamma-ray energy approaches several MeV and therefore pair production is predominantly confined to high-energy gamma rays. In the interaction (which must take place in the coulomb field of a nucleus), the gamma-ray photon disappears and is replaced by an electron–positron pair. All the excess energy carried in by the photon above the 1.02 MeV required to create the pair goes into kinetic energy shared by the positron and the electron. Because the positron will subsequently annihilate

†The simple analysis here neglects the atomic binding of the electron and assumes that the gamma-ray photon interacts with a free electron. If the small binding energy is taken into account, the unique energy of the scattered photon at a fixed angle predicted by Eq. 2.17 is spread into a narrow distribution centered about that energy (see Fig. 13.9).

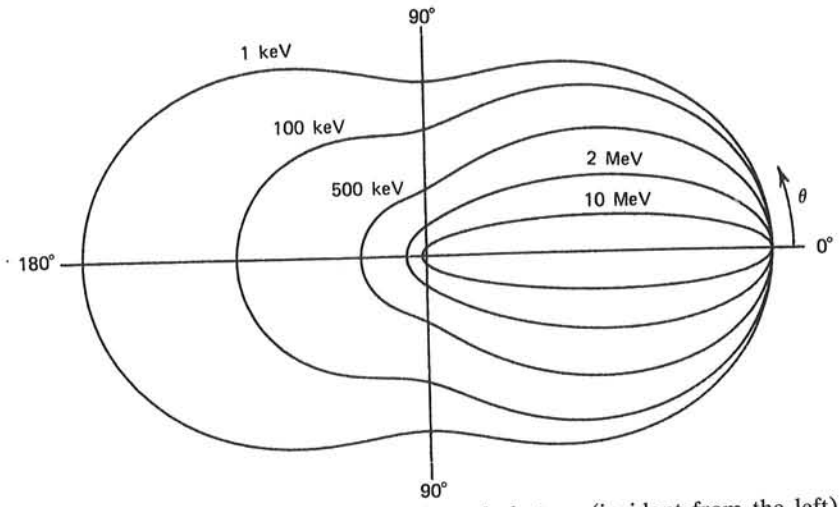

Figure 2.19 A polar plot of the number of photons (incident from the left) Compton scattered into a unit solid angle at the scattering angle θ. The curves are shown for the indicated initial energies.

after slowing down in the absorbing medium, two annihilation photons are normally produced as secondary products of the interaction. The subsequent fate of this annihilation radiation has an important effect on the response of gamma-ray detectors, as described in Chapter 10.

No simple expression exists for the probability of pair production per nucleus, but its magnitude varies approximately as the square of the absorber atomic number.[1] The importance of pair production rises sharply with energy, as indicated in Fig. 2.18.

The relative importance of the three processes described above for different absorber materials and gamma-ray energies is conveniently illustrated in Fig. 2.20. The line at the left represents the energy at which photoelectric absorption and Compton scattering are equally probable as a function of the absorber atomic number. The line at the right represents the energy at which Compton scattering and pair production are equally probable. Three areas are thus defined on the plot within which photoelectric absorption, Compton scattering, and pair production each predominate.

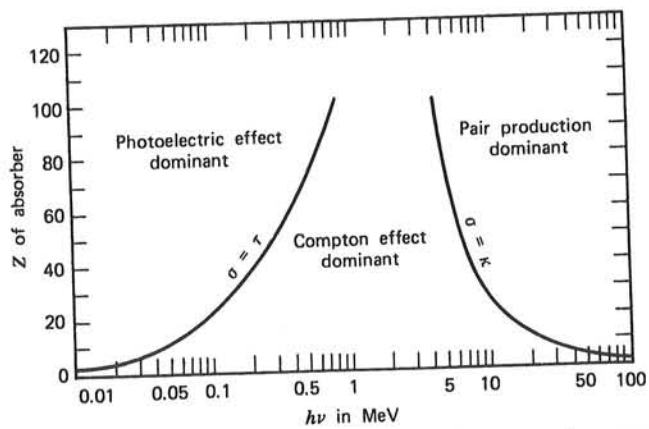

Figure 2.20 The relative importance of the three major types of gamma-ray interaction. The lines show the values of Z and $h\nu$ for which the two neighboring effects are just equal. (From *The Atomic Nucleus* by R. D. Evans. Copyright 1955 by the McGraw-Hill Book Company. Used with permission.)

4. COHERENT SCATTERING

In addition to Compton scattering, another type of scattering can occur in which the gamma-ray photon interacts coherently with all the electrons of an absorber atom. This *coherent scattering* or *Rayleigh scattering* process[1] neither excites nor ionizes the atom, and the gamma-ray photon retains its original energy after the scattering event. Because virtually no energy is transferred, this process is often neglected in basic discussions of gamma-ray interactions, and we will also ignore it in the discussions that follow. However, the direction of the photon is changed in coherent scattering, and complete models of gamma-ray transport must take it into account. The probability of coherent scattering is significant only for low photon energies (typically below a few hundred keV for common materials) and is most prominent in high-Z absorbers. The average deflection angle decreases with increasing energy, further restricting the practical importance of coherent scattering to low energies.

B. Gamma-Ray Attenuation

1. ATTENUATION COEFFICIENTS

If we again picture a transmission experiment as in Fig. 2.21, where monoenergetic gamma rays are collimated into a narrow beam and allowed to strike a detector after passing through an absorber of variable thickness, the result should be simple exponential attenuation of the gamma rays as also shown in Fig. 2.21. Each of the interaction processes removes the gamma-ray photon from the beam either by absorption or by scattering away from the detector direction and can be characterized by a fixed probability of occurrence per unit path length in the absorber. The sum of these probabilities is simply the probability per unit path length that the gamma-ray photon is removed from the beam:

$$\mu = \tau(\text{photoelectric}) + \sigma(\text{Compton}) + \kappa(\text{pair}) \tag{2.19}$$

and is called the *linear attenuation coefficient*. The number of transmitted photons I is then given in terms of the number without an absorber I_0 as

$$\frac{I}{I_0} = e^{-\mu t} \tag{2.20}$$

The gamma-ray photons can also be characterized by their *mean free path* λ, defined as the average distance traveled in the absorber before an interaction takes place. Its value can be obtained from

$$\lambda = \frac{\displaystyle\int_0^\infty x e^{-\mu x}\, dx}{\displaystyle\int_0^\infty e^{-\mu x}\, dx} = \frac{1}{\mu} \tag{2.21}$$

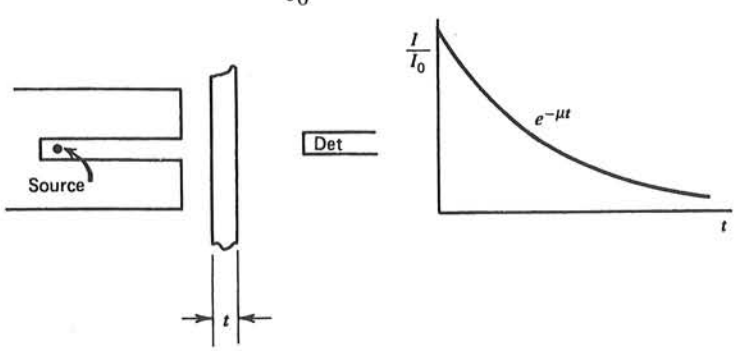

Figure 2.21 The exponential transmission curve for gamma rays measured under "good geometry" conditions.

and is simply the reciprocal of the linear attenuation coefficient. Typical values of λ range from a few mm to tens of cm in solids for common gamma-ray energies.

Use of the linear attenuation coefficient is limited by the fact that it varies with the density of the absorber, even though the absorber material is the same. Therefore, the *mass attenuation coefficient* is much more widely used and is defined as

$$\text{mass attenuation coefficient} = \frac{\mu}{\rho} \tag{2.22}$$

where ρ represents the density of the medium. For a given gamma-ray energy, the mass attenuation coefficient does not change with the physical state of a given absorber. For example, it is the same for water whether present in liquid or vapor form. The mass attenuation coefficient of a compound or mixture of elements can be calculated from

$$\left(\frac{\mu}{\rho}\right)_c = \sum_i w_i \left(\frac{\mu}{\rho}\right)_i \tag{2.23}$$

where the w_i factors represent the weight fraction of element i in the compound or mixture.

2. ABSORBER MASS THICKNESS

In terms of the mass attenuation coefficient, the attenuation law for gamma rays now takes the form

$$\frac{I}{I_0} = e^{-(\mu/\rho)\rho t} \tag{2.24}$$

The product ρt, known as the *mass thickness* of the absorber, is now the significant parameter that determines its degree of attenuation. Units of mass thickness have historically been mg/cm^2, and this convention is retained in this text. The thickness of absorbers used in radiation measurements is therefore often measured in mass thickness rather than physical thickness, because it is a more fundamental physical quantity.

The mass thickness is also a useful concept when discussing the energy loss of charged particles and fast electrons. For absorber materials with similar neutron/proton ratios, a particle will encounter about the same number of electrons passing through absorbers of equal mass thickness. Therefore, the stopping power and range, when expressed in units of ρt, are roughly the same for materials that do not differ greatly in Z.

3. BUILDUP

The gamma-ray attenuation experiment of Fig. 2.21, in which the gamma rays are collimated to a narrow beam before striking the absorber, is sometimes characterized as a "narrow beam" or "good geometry" measurement. The essential characteristic is that only gamma rays from the source that escape interaction in the absorber can be counted by the detector. Real measurements are often carried out under different circumstances (as sketched below) in which the severe collimation of the gamma rays is absent.

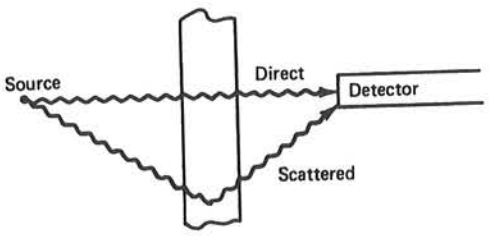

Now the detector can respond either to gamma rays directly from the source, to gamma rays that reach the detector after having scattered in the absorber, or to other types of secondary photon radiation. Many types of detectors will be unable to distinguish between these possibilities, so that the measured detector signal will be larger than that recorded under equivalent "good geometry" conditions. The conditions that lead to the simple exponential attenuation of Eq. (2.20) are therefore violated in this "broad beam" or "bad geometry" measurement because of the additional contribution of the secondary gamma rays. This situation is usually handled by replacing Eq. (2.20) by the following:

$$\frac{I}{I_0} = B(t, E_\gamma)e^{-\mu t} \tag{2.25}$$

where the factor $B(t, E_\gamma)$ is called the *buildup factor*. The exponential term is retained to describe the major variation of the gamma-ray counting rate with absorber thickness, and the buildup factor is introduced as a simple multiplicative correction. The magnitude of the buildup factor depends on the type of gamma-ray detector used, because this will affect the relative weight given to the direct and secondary gamma rays. (With a detector that responds only to the direct gamma rays, the buildup factor is unity.) The buildup also depends on the specific geometry of the experiment. As a rough rule of thumb, the buildup factor for thick slab absorbers tends to be about equal to the thickness of the absorber measured in units of mean free path of the incident gamma rays, provided the detector responds to a broad range of gamma-ray energies.

IV. INTERACTION OF NEUTRONS

A. General Properties

In common with gamma rays, neutrons carry no charge and therefore cannot interact in matter by means of the coulomb force, which dominates the energy loss mechanisms for charged particles and electrons. Neutrons can also travel through many centimeters of matter without any type of interaction and thus can be totally invisible to a detector of common size. When a neutron does undergo interaction, it is with a nucleus of the absorbing material. As a result of the interaction, the neutron may either totally disappear and be replaced by one or more secondary radiations, or else the energy or direction of the neutron is changed significantly.

In contrast to gamma rays, the secondary radiations resulting from neutron interactions are almost always heavy charged particles. These particles may be produced either as a result of neutron-induced nuclear reactions or they may be the nuclei of the absorbing material itself, which have gained energy as a result of neutron collisions. Most neutron detectors utilize some type of conversion of the incident neutron into secondary charged particles, which can then be detected directly. Specific examples of the most useful conversion processes are detailed in Chapters 14 and 15.

The relative probabilities of the various types of neutron interactions change dramatically with neutron energy. In somewhat of an oversimplification, we will divide neutrons into two categories on the basis of their energy, either "fast neutrons" or "slow neutrons," and discuss their interaction properties separately. The dividing line will be at about 0.5 eV, or about the energy of the abrupt drop in absorption cross section in cadmium (the *cadmium cutoff* energy).

B. Slow Neutron Interactions

For slow neutrons, the significant interactions include elastic scattering with absorber nuclei and a large set of neutron-induced nuclear reactions. Because of the small kinetic energy of slow neutrons, very little energy can be transferred to the nucleus in elastic scattering. Consequently, this is not an interaction on which detectors of slow neutrons can be based. Elastic collisions tend to be very probable, however, and often serve to bring the slow neutron into thermal equilibrium with the absorber medium before a different type of interaction takes place. Much of the population in the slow neutron energy range will therefore be found among these *thermal neutrons*, which, at room temperature, have an average energy of about 0.025 eV.

The slow neutron interactions of real importance are neutron-induced reactions that can create secondary radiations of sufficient energy to be detected directly. Because the incoming neutron energy is so low, all such reactions must have a positive Q-value to be energetically possible. In most materials, the radiative capture reaction [or (n, γ) reaction] is the most probable and plays an important part in the attenuation or shielding of neutrons. Radiative capture reactions can be useful in the indirect detection of neutrons using activation foils as described in Chapter 19, but they are not widely applied in active neutron detectors because the secondary radiation takes the form of gamma rays, which are also difficult to detect. Instead, reactions such as (n, α), (n, p), and (n, fission) are much more attractive because the secondary radiations are charged particles. A number of specific reactions of this type are detailed in Chapter 14.

C. Fast Neutron Interactions

The probability of most neutron–induced reactions potentially useful in detectors drops off rapidly with increasing neutron energy. The importance of scattering becomes greater, however, because the neutron can transfer an appreciable amount of energy in one collision. The secondary radiations in this case are *recoil nuclei*, which have picked up a detectable amount of energy from neutron collisions. At each scattering site, the neutron loses energy and is thereby *moderated* or slowed to lower energy. The most efficient moderator is hydrogen because the neutron can lose up to all its energy in a single collision with a hydrogen nucleus. For heavier nuclei, only a partial energy transfer is possible [see Eq.(15.4) and the associated discussion].

If the energy of the fast neutron is sufficiently high, *inelastic scattering* with nuclei can take place in which the recoil nucleus is elevated to one of its excited states during the collision. The nucleus quickly de-excites, emitting a gamma ray, and the neutron loses a greater fraction of its energy than it would in an equivalent elastic collision. Inelastic scattering and the subsequent secondary gamma rays play an important role in the shielding of high-energy neutrons but are an unwanted complication in the response of most fast neutron detectors based on elastic scattering.

D. Neutron Cross Sections

For neutrons of a fixed energy, the probability per unit path length is a constant for any one of the interaction mechanisms. It is conventional to express this probability in terms of the *cross section* σ per nucleus for each type of interaction. The cross section has units of area and has traditionally been measured in units of the *barn* (10^{-28} m^2). For example, each nuclear species will have an elastic scattering cross section, a radiative capture cross section, and so on, each of which will be a function of the neutron energy. Some examples of cross section plots are given in Figs. 14.1 and 14.2.

When multiplied by the number of nuclei N per unit volume, the cross section σ is converted into the macroscopic cross section Σ

$$\Sigma = N\sigma \tag{2.26}$$

which now has dimensions of inverse length. Σ has the physical interpretation of the probability per unit path length for the specific process described by the "microscopic" cross section σ. When all processes are combined by adding together the cross sections for each individual interaction

$$\Sigma_{\text{tot}} = \Sigma_{\text{scatter}} + \Sigma_{\text{rad. capture}} + \cdots \tag{2.27}$$

the resulting Σ_{tot} is the probability per unit path length that any type of interaction will occur. This quantity has the same significance for neutrons as the linear absorption coefficient for gamma rays defined earlier. If a narrow beam attenuation experiment is carried out for neutrons, as sketched earlier for gamma rays, the result will be the same: The number of detected neutrons will fall off exponentially with absorber thickness. In this case the attenuation relation is written

$$\frac{I}{I_0} = e^{-\Sigma_{\text{tot}} t} \tag{2.28}$$

The neutron mean free path λ is, by analogy with the gamma-ray case, given by $1/\Sigma_{\text{tot}}$. In solid materials, λ for slow neutrons may be of the order of a centimeter or less, whereas for fast neutrons, it is normally tens of centimeters.

Under most circumstances, neutrons are not narrowly collimated so that typical shielding situations involve broad beam or "bad geometry" conditions. Just as in the case of gamma rays, the exponential attenuation of Eq. (2.28) is no longer an adequate description because of the added importance of scattered neutrons reaching the detector. A more complex neutron transport computation is then required to predict the number of transmitted neutrons and their distribution in energy.

When discussing the rate of reactions induced by neutrons, it is convenient to introduce the concept of neutron flux. If we first consider neutrons with a single energy or fixed velocity v, the product $v\Sigma$ gives the interaction frequency for the process for which Σ is the macroscopic cross section. The reaction rate density (reactions per unit time and volume) is then given by $n(r)v\Sigma$, where $n(r)$ is the neutron number density at the vector position r, and $n(r)v$ is defined as the *neutron flux* $\varphi(r)$ with dimensions of length^{-2} time^{-1}. Thus, the reaction rate density is given by the product of the neutron flux and the macroscopic cross section for the reaction of interest:

$$\text{reaction rate density} = \varphi(r)\Sigma \tag{2.29}$$

This relation can be generalized to include an energy-dependent neutron flux $\varphi(r, E)$ and cross section $\Sigma(E)$:

$$\text{reaction rate density} = \int_0^\infty \varphi(r, E)\, \Sigma(E)\, dE \tag{2.30}$$

V. RADIATION EXPOSURE AND DOSE

Because of their importance in personnel protection at radiation-producing facilities and in the medical applications of radiation, the concepts of radiation exposure and dose play prominent roles in radiation measurements. In the following sections, we introduce the fundamental concepts that underlie the quantities and units of importance in this area. Precise definitions of quantities related to radiation protection are continually evolving, and the reader is referred to publications of the International Commission on Radiological Units and Measurements (ICRU), the International Commission on Radiological Protection (ICRP), and the U.S. National Commission on Radiation Protection (NCRP) for up-to-date information. As examples, Refs. 29 and 30 are comprehensive reviews of the units and detailed issues that arise in the monitoring of radiation exposures.

A. Gamma-Ray Exposure

The concept of gamma-ray exposure was introduced early in the history of radioisotope research. Defined only for sources of X- or gamma rays, a fixed exposure rate exists at every point in space surrounding a source of fixed intensity. The exposure is linear, in that doubling the source intensity also doubles the exposure rate everywhere around the source.

The basic unit of gamma-ray exposure is defined in terms of the charge dQ due to ionization created by the secondary electrons (negative electrons and positrons) formed within a volume element of air and mass dm, when these secondary electrons are completely stopped in air. The exposure value X is then given by dQ/dm. The SI unit of gamma-ray exposure is thus the coulomb per kilogram (C/kg), which has not been given a special name. The historical unit has been the *roentgen* (R), defined as the exposure that results in the generation of one electrostatic unit of charge (about 2.08×10^9 ion pairs) per 0.001293 g (1 cm^3 at STP) of air. The two units are related by

$$1\ \text{R} = 2.58 \times 10^{-4}\ \text{C/kg}$$

The exposure is therefore defined in terms of the effect of a given flux of gamma rays on a test volume of air and is a function only of the intensity of the source, the geometry between the source and test volume, and any attenuation of the gamma rays that may take place between the two. Its measurement fundamentally requires the determination of the charge due to ionization produced in air under specific conditions. Inherent in the above definition is the obligation to track each secondary electron created by primary gamma-ray interactions in the test volume under consideration, and to add up the ionization charges formed by that secondary electron until it reaches the end of its path. This requirement is often difficult or impossible to achieve in actual practice, and therefore instruments that are designed to measure gamma-ray exposure usually employ approximations that involve the principle of compensation introduced in Chapter 5.

The gamma-ray exposure, although not directly tied to physical phenomena, is often of interest in gamma-ray dosimetry. It is therefore often convenient to be able to calculate the exposure rate at a known distance from a point radioisotope source. If we assume that the yield per disintegration of X- and gamma rays is accurately known for the radioisotope of interest, the exposure per unit activity of the source at a known distance can simply be expressed under the following conditions:

1. The source is sufficiently small so that spherical geometry holds (i.e., the photon flux diminishes as $1/d^2$, where d is the distance to the source).
2. No attenuation of the X- or gamma rays takes place in the air or other material between the source and measuring point.
3. Only photons passing directly from the source to the measuring point contribute to the exposure, and any gamma rays scattered in surrounding materials may be neglected.

The exposure rate $\dot{X}$ is then

$$\dot{X} = \Gamma_\delta \frac{\alpha}{d^2} \tag{2.31}$$

where α is the activity of the source, and Γ_δ is defined as the *exposure rate constant* for the specific radioisotope of interest. The subscript δ implies that the assumption has been made that all X- and gamma rays emitted by the source above an energy δ contribute to the dose, whereas those below this energy are not sufficiently penetrating to be of practical interest. The value of Γ_δ for a particular radioisotope can be calculated from its gamma-ray yield and the energy-dependent absorption properties of air. Some particular values for $\delta = 0$ are listed in Table 2.1.

Table 2.1 Exposure Rate Constant for Some Common Radioisotope Gamma-Ray Sources

Nuclide	Γ^a
Antimony-124	9.8
Cesium-137	3.3
Cobalt-57	0.9
Cobalt-60	13.2
Iodine-125	~0.7
Iodine-131	2.2
Manganese-54	4.7
Radium-226	8.25
Sodium-22	12.0
Sodium-24	18.4
Technetium-99m	1.2
Zinc-65	2.7

[a]The exposure rate constant Γ is in units of $(R \cdot cm^2)/(hr \cdot mCi)$.

Source: The Health Physics and Radiological Health Handbook, Nucleon Lectern Associates, Olney, MD, 1984.

B. Absorbed Dose

Two different materials, if subjected to the same gamma-ray exposure, will in general absorb different amounts of energy. Because many important phenomena, including changes in physical properties or induced chemical reactions, would be expected to scale as the energy absorbed per unit mass of the material, a unit that measures this quantity is of fundamental interest. The energy absorbed from any type of radiation per unit mass of the absorber is defined as the *absorbed dose*. The historical unit of absorbed dose has been the *rad*, defined as 100 ergs/gram. As with other historical radiation units, the rad is being gradually replaced by its SI equivalent, the *gray* (Gy) defined as 1 joule/kilogram. The two units are therefore simply related by:

$$1 \text{ Gy} = 100 \text{ rad}$$

The absorbed dose should be a reasonable measure of the chemical or physical effects created by a given radiation exposure in an absorbing material. Careful measurements have shown that the absorbed dose in air corresponding to a gamma-ray exposure of 1 coulomb/kilogram amounts to 33.8 joules/kilogram, or 33.8 Gy. If water is substituted for the air, its absorption properties per unit mass do not differ greatly because the average atomic number of water is much the same as that of air. For absorbing materials of greatly dissimilar atomic numbers, however, the interaction mechanisms have different relative importance, and therefore the absorbed dose per unit exposure would show greater differences.

In order to measure absorbed dose in a fundamental manner, some type of energy measurement must be carried out. One possibility is a calorimetric measurement in which the rate of rise of the temperature in a sample of absorber is used to calculate the rate of energy deposition per unit mass. Because of their difficulty, these measurements are not commonplace for routine application since the thermal effects created even by large doses

of radiation are very small. Instead, indirect measurements of absorbed dose are much more common, in which its magnitude is inferred from ionization measurements carried out under proper conditions (see Chapter 5).

C. Dose Equivalent

When the effects of radiation on living organisms are evaluated, the absorption of equal amounts of energy per unit mass under different irradiation conditions does not guarantee the same biological effect. In fact, the extent of the effects can differ by as much as an order of magnitude depending on whether the energy is deposited in the form of heavy charged particles or electrons.

The biological damage created by ionizing radiation is traceable to the chemical alteration of the biological molecules that are influenced by the ionization or excitation caused by the radiation. The severity and permanence of these changes are directly related to the local rate of energy deposition along the particle track, known as the *linear energy transfer*† L. Those radiations with large values of L (such as heavy charged particles) tend to result in greater biological damage than those with lower L (such as electrons), even though the total energy deposited per unit mass is the same.

The concept of *dose equivalent* has therefore been introduced to more adequately quantify the probable biological effect of the given radiation exposure. A unit of dose equivalent is defined as that amount of any type of radiation that, when absorbed in a biological system, results in the same biological effect as one unit of absorbed dose delivered in the form of low-L radiation. The dose equivalent H is the product of the absorbed dose D and the *quality factor* Q that characterizes the specific radiation:

$$H = DQ \tag{2.32}$$

The quality factor increases with linear energy transfer L as shown in Table 2.2.

For the fast electron radiations of interest in this text, L is sufficiently low so that Q is essentially unity in all applications. Therefore, the dose equivalent is numerically equal to the absorbed dose for beta particles or other fast electrons. The same is true for X-rays and gamma rays because their energy is also delivered in the form of fast secondary electrons. Charged particles have a much higher linear energy transfer and the dose equivalent is larger than the absorbed dose. For example, Q is approximately 20 for alpha particles of typical energies. Because neutrons deliver most of their energy in the form of heavy

Table 2.2 Quality Factors for Different Radiations

L in Water (keV/μm)	Q
< 10	1
10–100	$0.32L - 2.2$
> 100	$300/\sqrt{L}$

From ICRP Publication 60.

†The linear energy transfer is nearly identical to the specific energy loss ($-dE/dx$) defined earlier. The only differences arise when a substantial portion of the radiation energy is liberated in the form of bremsstrahlung, which may travel a substantial distance from the particle track before depositing its energy. The specific energy loss includes the bremsstrahlung as part of the energy loss of the particle, but the linear energy transfer L counts only the energy that is deposited along the track and therefore excludes the bremsstrahlung.

charged particles, their effective quality factor is also considerably greater than unity and varies significantly with the neutron energy.

The units used for dose equivalent H depend on the corresponding units of absorbed dose D in Eq. (2.32). If D is expressed in the historical unit of the rad, H is defined to be in units of the *rem*. Historically, the rem (or millirem) was universally used to quantify dose equivalent. Under the SI convention, D is instead expressed in grays, and a corresponding unit of dose equivalent called the *sievert* (Sv) has been introduced. For example, an absorbed dose of 2 Gy delivered by radiation with Q of 5 will result in a dose equivalent of 10 Sv. Because 1 Gy = 100 rad, the units are interrelated by

$$1 \text{ Sv} = 100 \text{ rem}$$

Guidelines for radiation exposure limits to personnel are quoted in units of dose equivalent in order to place exposures to different types and energies of radiation on a common basis.

D. Fluence-to-Dose Conversion

For neutrons and gamma rays that are relatively penetrating radiations, it is sometimes convenient to be able to estimate the dose equivalent to exposed personnel that results from a given *fluence* of the radiation. The fluence is generally defined as $\Phi = dN/da$ where dN represents the differential number of gamma-ray photons or neutrons that are incident on a sphere with differential cross-sectional area da. In terms of the neutron flux defined on p. 57, the fluence is the time integral of the flux over the exposure duration. For a monodirectional beam, the fluence is simply the number of photons or neutrons per unit area, where the area is perpendicular to the direction of the beam. The number of counts recorded from typical radiation detectors is most easily interpreted in terms of the number of radiation-induced interactions in the detector, and therefore is more closely related to fluence than to dose. A conversion between fluence and dose can therefore be helpful in interpreting measurements made using specific detectors.

Because the attenuation of gamma rays or fast neutrons in air is negligible over small distances, the direct (or unscattered) fluence often can be estimated from point sources by assuming that $\Phi = N/4\pi d^2$, where N is the number of photons or neutrons emitted by the source and d is the distance from the source. More complicated geometries require the use of radiation transport codes to predict the fluence and energy spectrum at a given location.

The conversion from fluence to dose must take into account the energy-dependent probabilities of producing ionizing secondary particles from gamma-ray and/or neutron interactions, the kinetic energy that is deposited by these particles, and the quality factor Q that should be applied to convert deposited energy per unit mass to dose equivalent. By assuming a physical model for the human body, gamma-ray and neutron transport codes can be applied to calculate energy deposition and dose for the various tissues and organ systems. These calculations will be sensitive to the direction of incidence of the radiation because of self-shielding and attenuation effects within the body. Taking into account the differing radiosensitivity of various organs and tissues through the tissue-weighting factors recommended by the ICRP (see following section), the individual dose components can then be combined into an *effective dose equivalent* H_E (see Ref. 31) to represent an estimate of the overall biological effect of a uniform, whole body exposure to the assumed fluence. The effective dose equivalent is then written as

$$H_E = h_E \Phi \tag{2.33}$$

where h_E is the fluence-to-dose factor. Values of h_E for gamma rays and neutrons are plotted as a function of energy in Fig. 2.22.

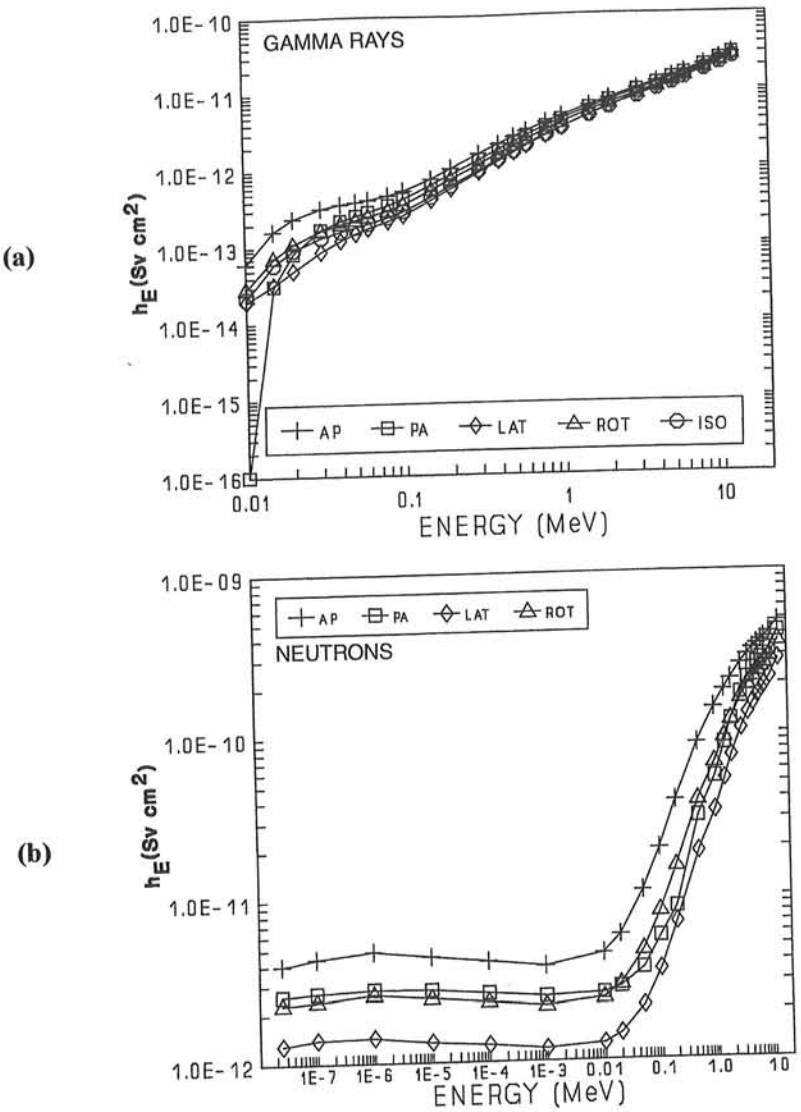

Figure 2.22 Fluence-to-dose conversion factors h_E for uniform whole body exposures to (*a*) gamma rays and (*b*) neutrons. The labels refer to different assumed directions of the incident particle flux: AP for frontal exposure of the body, PA for rear exposure, LAT for exposure from the side, ROT for uniform rotation of the body about its axis, perpendicular to the directional flux, and ISO for an isotropic incident flux. Tabulated data and additional details are given in Ref. 31, which is the source of these data. (Copyright 1992 by the American Nuclear Society, LaGrange Park, Illinois.)

E. ICRP Dose Units

In its report ICRP Publication 60, the International Commission on Radiation Protection has introduced a somewhat different set of definitions that are also used in the radiation protection literature. A new quantity is named the *equivalent dose* and given the symbol $H_{T,R.}$. It is obtained from the absorbed dose $D_{T,R}$ averaged over a tissue or organ T due to radiation R, multiplied by a radiation weighting factor w_R that accounts for the different biological effects of various radiations:

$$H_{T,R} = w_R \cdot D_{T,R} \tag{2.34}$$

Table 2.3 Radiation Weighting Factors

Type and Energy Range	Radiation Weighting Factor, w_R
Photons, all energies	1
Electrons and muons, all energies	1
Neutrons, energy < 10 keV	5
10 keV to 100 keV	10
> 100 keV to 2 MeV	20
> 2 MeV to 20 MeV	10
> 20 Me V	5
Protons, other than recoil protons, energy > 2 MeV	5
Alpha particles, fission fragments, heavy nuclei	20

From ICRP Publication 60.

Values of w_R are shown in Table 2.3. Units for equivalent dose are sieverts when the absorbed dose is expressed in grays. If there is a mix of radiations, then the total equivalent dose H_T is given by a sum over all radiation types:

$$H_T = \sum_R H_{T,R} = \sum_R w_R \cdot D_{T,R} \tag{2.35}$$

To account for the differing radiosensitivity of various organs and tissues, a set of tissue-weighting factors w_T are introduced to allow calculation of what is now called the *effective dose E:*

$$E = \sum_T w_T \cdot H_T \tag{2.36}$$

This quantity is intended to fill the same role as the effective dose equivalent H_E described in the previous section, in that it is an estimate of the overall effect of a given exposure to radiation. The tissue-weighting factors are chosen to give greater weight to those organs and tissues that are most sensitive to radiation. The factors are normalized in that their sum is unity, so that a uniform equivalent dose H_T to the whole body of one sievert will result in an effective dose E of one sievert. Recommended values for the tissue-weighting factors can be found in ICRP Publication 60.

It should be emphasized that the estimation of the effect of a given exposure to ionizing radiation is by its very nature an inexact science.[32] Biological effects are not absolute physical quantities that can be measured with high precision. The concepts of effective dose or effective dose equivalent are intended only to provide guidance in approximating the potential effects of a given exposure to radiation and should not be regarded as highly accurate or exactly reproducible quantities.

PROBLEMS

2.1 Estimate the time required for a 5 MeV alpha particle to slow down and stop in silicon. Repeat for the same particle in hydrogen gas.

2.2 With the aid of Fig. 2.7, estimate the energy remaining in a beam of 5 MeV protons after passing through 100 μm of silicon.

2.3 Using Fig. 2.10, find the approximate energy loss of 1 MeV alpha particles in a thickness of 5 μm of gold.

2.4 Estimate the range of 1 MeV electrons in aluminum with the aid of Fig. 2.14.

2.5 Calculate the energy of a 1 MeV gamma-ray photon after Compton scattering through 90°.

2.6 Give a rough estimate of the ratio of the probability per atom for photoelectric absorption in silicon to that in germanium.

2.7 Indicate which of the three major interaction processes (photoelectric absorption, Compton scattering, pair production) is dominant in the following situations:

(a) 1 MeV gamma rays in aluminum.

(b) 100 keV gamma rays in hydrogen.

(c) 100 keV gamma rays in iron.

(d) 10 MeV gamma rays in carbon.

(e) 10 MeV gamma rays in lead.

2.8 **(a)** From Fig. 2.18, calculate the mean free path of 1 MeV gamma rays in sodium iodide (specific gravity = 3.67).

(b) What is the probability that a 600 keV gamma ray undergoes photoelectric absorption in 1 cm of sodium iodide?

2.9 Define the following terms:

(a) Absorber mass thickness.

(b) Buildup.

(c) Neutron inelastic scattering.

(d) Macroscopic cross section.

(e) Neutron flux.

2.10 For 140 keV gamma rays, the mass attenuation coefficients for hydrogen and oxygen are 0.26 and 0.14 cm^2/g, respectively. What is the mean free path in water at this energy?

2.11 How many 5 MeV alpha particles are required to deposit a total energy of 1 J?

2.12 A beam of 1 MeV electrons strikes a thick target. For a beam current of 100 microamperes (μA), find the power dissipated in the target.

2.13 Using the data in Table 2.1, estimate the exposure rate 5 m from a 1-Ci source of ^{60}Co.

2.14 Calculate the rate of temperature rise in a sample of liquid water adiabatically exposed to radiation that results in an absorbed dose rate of 10 mrad/h.

2.15 Using the data in Fig. 2.22*b*, estimate the effective dose equivalent to an individual who spends an 8-hour day working at an average distance of 5 m from a 3 μg ^{252}Cf fast neutron source (see discussion of spontaneous fission sources in Chapter 1).

REFERENCES

1. R. D. Evans, *The Atomic Nucleus*, Krieger, New York, 1982.
2. A. Beiser, *Revs. Mod. Phys.* **24**, 273 (1952).
3. B. Wilken and T. A. Fritz, *Nucl. Instrum. Meth.* **138**, 331 (1976).
4. D. J. Skyrme, *Nucl. Instrum. Meth.* **57**, 61 (1967).
5. C.F. Williamson, J. P. Boujot, and J. Picard, CEA-R3042 (1966).
6. C. Hanke and J. Laursen, *Nucl. Instrum. Meth.* **151**, 253 (1978).
7. W. H. Barkas and M. J. Berger, National Academy of Sciences, National Research Council, Publications 1133, 103 (1964).
8. L. C. Northcliffe and R. F. Schilling, *Nuclear Data Tables*, **A7**, 233 (1970).
9. J. F. Ziegler, *The Stopping and Ranges of Ions in Matter*, Pergamon Press, New York, 1977.
10. "Stopping Powers and Ranges for Protons and Alpha Particles," ICRU Report 49, ICRU, Bethesda (1993).
11. G. Cesini, G. Lucarini, and F. Rustichelli, *Nucl. Instrum. Meth.* **127**, 579 (1975).
12. P. D. Bourland and D. Powers, *Phys. Rev. B* **3**, 3635 (1971).
13. J. S.-Y. Feng, W. K. Chu, and M-A. Nicolet, *Phys. Rev. B* **10**, 3781 (1974).
14. S. Matteson, E. K. L. Chau, and D. Powers, *Phys. Rev. A* **14**, 169 (1976).
15. D. I. Thwaites, *Nucl. Instrum. Meth.* **B69**, 53 (1992).
16. S. Saro et al., *Nucl. Instrum. Meth.* **A381**, 520 (1996).
17. A. Akkerman, et al., *J. Appl. Phys.* **76** (8), 4656 (1994).
18. Y. K. Dewaraja, R. F. Fleming, M. A. Ludington, and R. H. Fleming, *IEEE Trans. Nucl. Sci.* **41 (4)**, 871 (1994).
19. A. Breskin, *Nucl. Phys. B (Proc. Suppl.)* **44**, 351 (1995).
20. T. Odenweller, et al., *Nucl. Instrum. Meth.* **198**, 263 (1982).
21. W. Starzecki, A. M. Stefanini, S. Lunardi, and C. Signorini, *Nucl. Instrum. Meth.* **193**, 499 (1982).
22. M. J. Berger and S. M. Seltzer, National Bureau Of Standards Publication NBSIR 82-2550-A (1982).
23. L. Pages et al., *Atomic Data* **4**, 1 (1972).
24. T. Mukoyama, *Nucl. Instrum. Meth.* **134**, 125 (1976).
25. T. Baltakmens, *Nucl. Instrum. Meth.* **82**, 264 (1970).
26. T. Baltakmens, *Nucl. Instrum. Meth.* **142**, 535 (1977).
27. T. Tabata, R. Ito, and S. Okabe, *Nucl. Instrum. Meth.* **94**, 509 (1971).
28. G. Zavattini et al., *Nucl. Instrum. Meth.* **A401**, 206 (1997).
29. "1990 Recommendations of the International Commission on Radiological Protection," ICRP Publication 60, Pergamon Press, Oxford (1991).
30. "Quantities and Units in Radiation Protection Dosimetry," ICRU Report 51, ICRU, Bethesda (1993).
31. "Neutron and Gamma-Ray Fluence-to-Dose Factors," American National Standard ANSI/ANS-6.1.1-1991.
32. W. K. Sinclair, *Health Phys.* **70(6)**, 781 (1996).